Electronic Supplementary Information for

"Perfecting" pure shift HSQC: full homodecoupling for accurate and precise determination of heteronuclear couplings

Lukas Kaltschnee,[a] Andreas Kolmer,[a] István Timári,[b] Volker Schmidts,[a] Ralph W. Adams,[c] Mathias Nilsson,[c,d] Katalin E. Kövér,[b] Gareth A. Morris,[c] and Christina M. Thiele[,a]*

[a] *Clemens-Schöpf-Institut für Organische Chemie und Biochemie, Technische Universität Darmstadt, Alarich-Weiss-Straße 16, D-64287 Darmstadt, Germany. E-mail: cthiele@thielelab.de; Tel: +49 (0)6151 165112*

[b] *Department of Inorganic and Analytical Chemistry, University of Debrecen, Egyetem tér 1, H-4032 Debrecen, Hungary.*

[c] *School of Chemistry, University of Manchester, Oxford Road, Manchester M13 9PL, United Kingdom.*

[d] *Department of Food Science, University of Copenhagen, Rolighedsvej 30, DK-1958 Fredriksberg C, Denmark.*

Supporting Information

Table of Contents

Table of Contents 1

Preparation of (+)-Isopinocampheol samples 2

Data acquisition and processing 2

Instrumentation: 2

Pulse calibration for (+)-Isopinocampheol: 2

Settings used for all measurements on (+)-Isopinocampheol: 2

Measurements on (+)-Isopinocampheol in isotropic phase: 3

Measurements on (+)-Isopinocampheol in anisotropic phase: 3

Data processing: 3

Coupling constant extraction: 3

Coupling constant analysis: 3

F_2-coupled spectra measured at 600 MHz proton frequency, not shown in the main article 4

F_2-coupled spectra measured at 400 MHz proton frequency 5

Coordinates for (+)-IPC 7

Evaluation of the accuracy and precision of one-bond coupling constant extraction from BIRD and perfectBIRD decoupled spectra 8

Accuracy of one-bond coupling constant measurements in a two spin-1/2 system – experiments on $CHCl_3$ 8

Precision of one-bond coupling constant measurements in coupled spin systems – measurements on (+)-IPC 11

Coupling constants extracted from spectra collected at 600 MHz proton resonance frequency for (+)-Isopinocampheol 15

Quality factors 16

Comparison between experimental and back calculated RDCs 17

Output files generated by RDC@hotFCHT 18

F_2 coupled CLIP HSQC without homonuclear decoupling 18

F_2 coupled CLIP HSQC with BIRD decoupling 19

F_2 coupled CLIP HSQC with perfectBIRD decoupling 20

F_2 coupled CLAP HSQC without homonuclear decoupling 21

F_2 coupled CLAP HSQC with BIRD decoupling 22

F_2 coupled CLIP HSQC with perfectBIRD decoupling 23

Signal appearance in the case of strongly coupled spin systems 24

Pulse sequences for the F_2 heteronuclear coupled experiments presented 26

F_2 heteronuclear coupled F_2 perfectBIRD homodecoupled CLIP HSQC experiment 26

F_2 heteronuclear coupled F_2 perfectBIRD homodecoupled CLAP HSQC experiment 30

F_2 heteronuclear coupled F_2 BIRD homodecoupled CLIP HSQC experiment 33

F_2 heteronuclear coupled F_2 BIRD homodecoupled CLAP HSQC experiment 37

Spectra collected with $t'_2 = 0$ at 400 MHz proton frequency 40

Literature 41

Preparation of (+)-Isopinocampheol samples

(+)-Isopinocampheol obtained from Sigma Aldrich and CD_2Cl_2 obtained from Euriso-Top were used without further purification. High molecular weight PBDG (poly-γ-benzyl-D-glutamate) (Mw: $2.54 \cdot 10^6$ g/mol, PDI: 1.45) was prepared in house as previously described[1] for PBLG (poly-γ-benzyl-L-glutamate). The isotropic sample was prepared from 145.4 mg (+)-IPC and 644.2 mg CD_2Cl_2, while the anisotropic sample was prepared from 148.9 mg (+)-IPC, 78.8 mg PBDG (9.05 %-wt) and 643.1 mg CD_2Cl_2. The samples were degassed using a freeze pump thaw cycle and sealed under vacuum. The anisotropic sample was centrifuged back and forth for homogenization before use. The deuterium splitting observed was stable over the full lifetime of the sample, exceeding six months, with deuterium linewidths (full width at half height) below 2 Hz during all measurements, as checked using ^{2}H spectra.

Data acquisition and processing

Instrumentation:

Measurements at 14.1 T field strength (600.3 MHz ^{1}H frequency) were performed on an Avance III narrow bore system (Bruker Biospin, Karlsruhe) equipped with a 5 mm triple-band inverse probe (^{1}H, ^{2}H, ^{31}P, BB) with z-gradient. The maximum z-gradient strength was experimentally determined to be (0.494 ± 0.007) T m^{-1} using a stimulated echo experiment on a doped water sample. Gradient strengths are given as a fraction of this maximum amplitude. Sample temperature was held constant for all measurements using a BCU-Xtreme chiller (Bruker Biospin, Karlsruhe) at 300 K, unless otherwise stated. TopSpin 3.2 patchlevel 1 was used for acquisition, unless otherwise stated.

Measurements at 9.4 T field strength (400.1 MHz ^{1}H frequency) were performed on a DRX/II narrow bore system (Bruker Biospin, Karlsruhe) equipped with a 5 mm QNP probe (^{1}H, ^{2}H, ^{13}C/^{31}P/^{19}F) with z-gradient. The maximum z-gradient strength was experimentally determined to be (0.531 ± 0.008) T m^{-1} using the above-mentioned calibration procedure. Gradient strengths are given as a fraction of this maximum amplitude. Temperature was controlled at 300 K by a BCU 05 chiller. During acquisition, TopSpin 1.3 patchlevel 10 was used to control this instrument.

On both systems the temperature calibration at 300 K had been verified previous to the measurements using a methanol temperature calibration sample.

Pulse calibration for (+)-Isopinocampheol:

Previous to the coupling constant measurements pulse lengths and power were determined as follows: Hard proton pulses were calibrated in a simple proton experiment using the isotropic (+)-IPC sample by determination of the 360° pulse length. 90° pulse lengths of 9.13 µs and 12.5 µs were determined for the 14.1 T and the 9.4 T systems respectively. Hard 90° carbon pulse lengths of 13 µs and 9 µs were determined for the 14.1 T and the 9.4 T system respectively using a 0.1 M ^{15}N-labeled urea sample containing 0.1 M ^{13}C-labeled methanol in DMSO-d_6 at the 14.1 T system and using the isotropic (+)-IPC sample at the 9.4 T system. For measurements at 14.1 T, the attenuations used for chirp pulses were calculated using the TopSpin integrated ShapeTool software. The 9.4 T system does not provide a linearized pulse attenuator, therefore chirp pulses were calibrated manually using a heteronuclear multiple quantum experiment (dec180sp, Bruker pulse program library) and the above-mentioned labeled urea/methanol sample. The pulse settings given were used both for the measurements using the isotropic and for the anisotropic sample.

Settings used for all measurements on (+)-Isopinocampheol:

All spectra shown were acquired with spectral widths of 10.4 ppm (DW = 80 µs at 14.1 T and DW = 120 µs at 9.4 T) in the ^{1}H and 70 ppm in the ^{13}C dimension. Experiments without homonuclear decoupling were recorded in all cases with 8192 complex points in the proton dimension (FID sampling for 1.3 s at 14.1 T and for 2.0 s at 9.4 T), while varying settings were used for the experiments with homonuclear decoupling. 128 linearly sampled points were collected in the indirect dimension of all spectra using Echo-Antiecho gradient encoding. In all cases a two-step phase cycle (one scan per phase cycling step), 16 dummy scans and a recycle delay of 1 s were used. The delays d_1 and d_3 were optimized for $^1J_{CH}$ = 125 Hz. As indicated in Figure 1 of the main text, ^{13}C inversion and refocusing pulses were partially replaced by smoothed linear Chirp (60 kHz total sweep width, 0.5 ms length, 20 % smoothing, sweep from high to low field, Crp60,0.5,20.1) and smoothed Chirp composite pulses (60 kHz total sweep width, 2.0 ms length, four chirp composite pulse, Crp60comp.4) on both instruments. All gradient pulses used a smoothed square shape (SMSQ10.100) with an integration factor of 0.9 and a length of 1 ms and were followed by a recovery delay of 200 µs. The gradients strengths used were G_1 = 15 %, G_2 = 80 %, G_3 = 11 %, G_4 = 20.1 %, G_5 = 8 %, G_6 = 17 % and G_7 = (95 % at 9.4 T, 90 % at 14.1 T) of the above-mentioned maximum gradient strengths. The sign of G_2 was changed in alternate experiments according to the Echo-Antiecho procedure, to achieve F_1 sign

discrimination in the ^{13}C dimension. CLIP/CLAP HSQC experiments without homonuclear decoupling, as proposed by Luy *et al.*[2], only use G_2 and G_4.

Measurements on (+)-Isopinocampheol in isotropic phase:

For homodecoupled experiments, data collection was performed in small chunks of 1/(*sw*2) in length. At 14.1 T this chunk length was set to 15.36 ms (192 • direct acquisition dwell time, *sw*2 = 65.1 Hz) and 64 chunks were collected, resulting in a constructed FID of 1.0 s (6144 complex points). At 9.4 T 48 chunks of 19.20 ms length (160 • direct acquisition dwell time, *sw*2 = 52.1 Hz) were acquired, yielding a constructed FID of 0.9 s (3840 complex points).

Measurements on (+)-Isopinocampheol in anisotropic phase:

To cover the range of homonuclear coupling constants present in the aligned sample, 1/(*sw*2) was decreased as compared to the settings we used in the isotropic sample. We collected 32 chunks of data, each of 10.24 ms length (128 • direct acquisition dwell time, *sw*2 = 97.7 Hz) on the 14.1 T system to sample the FID in the proton dimension for 0.33 s (2048 complex data points). On the 9.4 T instrument 32 data chunks of 10.08 ms length (84 • direct acquisition dwell time, *sw*2 = 99.2 Hz) were accumulated to cover an overall acquisition time of 0.32 s (1344 complex data points). On both systems the resulting acquisition lengths were sufficient to sample the FID during its entire decay to below noise level, resulting in shorter experiment durations for the spectra measured for the aligned sample.

Data processing:

Spectra used for coupling constant extraction were all processed as follows: in the direct dimension data was zero-filled to 8192 complex data points prior to Fourier transformation. No window functions were applied in this dimension, to avoid any masking of decoupling artifacts. In the indirect dimension, the spectra were zero-filled to 256 points and multiplied by a 90° shifted squared sine function prior to Fourier transformation. Manual phasing was applied. The data presented has not been subjected to baseline correction. The F_2 traces shown for the different experiments as inserts in the figures show the data at the same noise level, as determined in an empty spectral region.

TopSpin 3.1 patchlevel 1 and TopSpin 3.2 patchlevel 6 were used for processing.

Coupling constant extraction:

Coupling constants were extracted using traces taken along the proton dimension at the respective ^{13}C frequencies. An inverse Fourier transform was applied to the data, which was then zero filled to 8192 complex points, Fourier transformed and duplicated. The duplicated traces were overlaid and shifted manually with respect to each other to determine the position of best overlap between the two peaks composing the heteronuclear doublet, in order to obtain the desired coupling constant. The traces were then shifted around this optimum position to estimate the maximum deviation from this position according to the procedure described in ref. [3]. In the case of antiphase doublets of CLAP experiments, a 180° 0^{th} order phase correction was applied to one of the traces overlaid before coupling constant extraction.

Coupling constant analysis:

From the total couplings $^1T_{CH}$ observed for the weakly aligned analyte, the RDCs $^1D_{CH}$ were calculated according to $^1T_{CH} = {}^1J_{CH} + 2\,{}^1D_{CH}$, where $^1J_{CH}$ is the scalar coupling constant observed in the isotropic solution. Using the program RDC@hotFCHT[4] the alignment tensor was calculated for the analyte in a single conformer single tensor fit[5]. The structural model used for (+)-IPC is given in the section “Coordinates for (+)-IPC”. During the evaluation of the alignment tensors no error weighting of the experimental RDCs was used. Using these alignment tensors, RDCs expected for the input structure were back-calculated. These back-calculated RDCs are compared with those determined experimentally in the section “Comparison between experimental and back calculated RDCs”.

F_2-coupled spectra measured at 600 MHz proton frequency, not shown in the main article

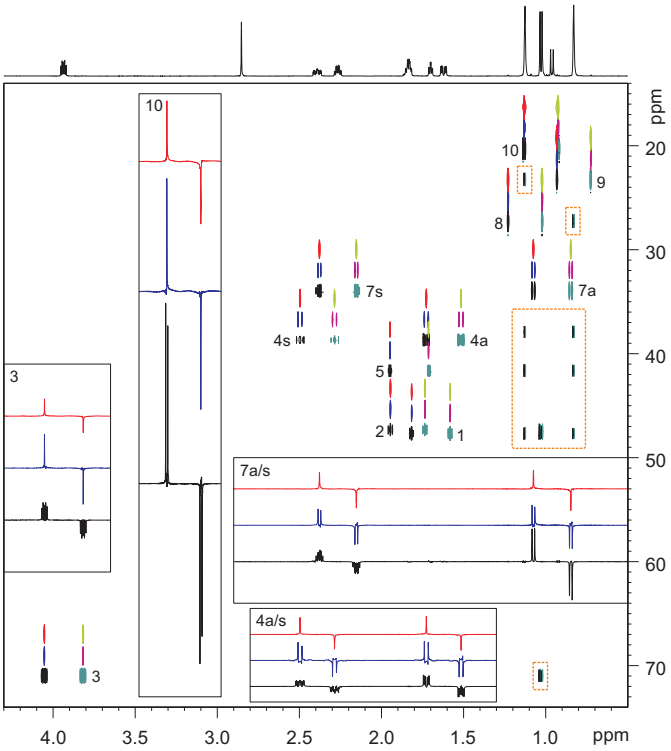

Figure S1: F_2-coupled CLAP HSQC spectra without homonuclear decoupling (pos. black, neg. cyan), with BIRD (pos. blue, neg. magenta) and with perfectBIRD (pos. red, neg. green) homonuclear decoupling during acquisition, collected for (+)-IPC in isotropic CD_2Cl_2 –solution at 14.1 T. Experimental durations were 10.5 min, 7.1 h and 9.4 h respectively. For selected protons, traces along the proton dimension are shown. The decoupled spectra are shifted in the carbon dimension for easier comparison. Signals arising in the CLAP HSQC without homonuclear decoupling due to long-range heteronuclear couplings (highlighted by dashed boxes) are suppressed by the homodecoupling as well.

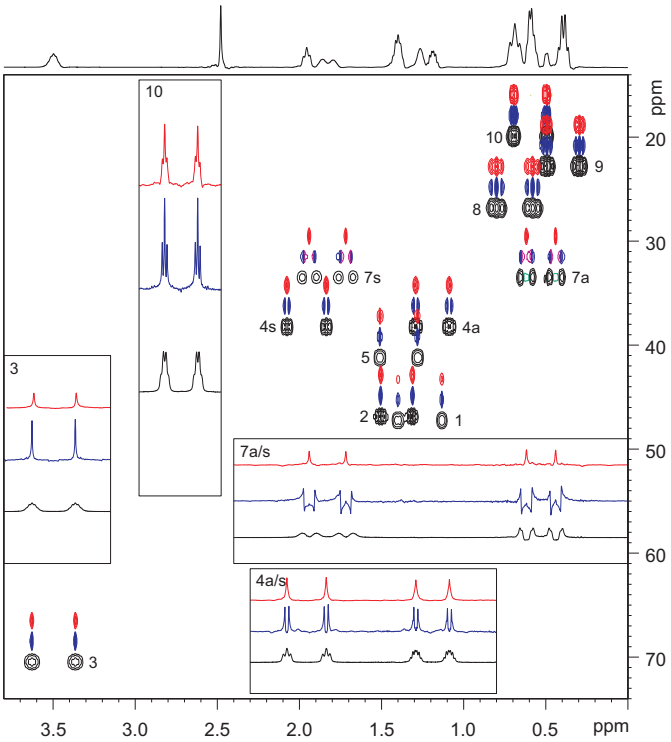

Figure S2: F_2-coupled CLIP HSQC spectra without homonuclear decoupling (black), with BIRD (blue) and with perfectBIRD (red) homonuclear decoupling during acquisition, collected for (+)-IPC in anisotropic CD_2Cl_2/PBDG-solution at 14.1 T. Experimental durations were 10.5 min, 2.8 h and 3.2 h respectively. For selected protons, traces along the proton dimension are shown. The decoupled spectra are shifted in the carbon dimension for easier comparison.

F_2-coupled spectra measured at 400 MHz proton frequency

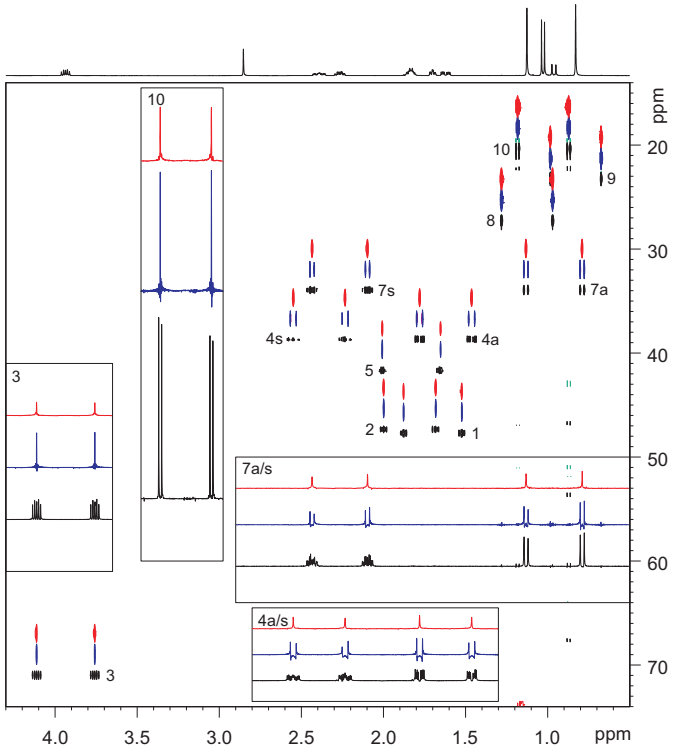

Figure S3: F_2-coupled CLIP HSQC spectra without homonuclear decoupling, with BIRD and with perfectBIRD homonuclear decoupling during acquisition, collected for (+)-IPC in isotropic CD_2Cl_2-solution at 9.4 T. The same color coding is used as in Figure S2. Experimental durations were 13.2 min (half duration of dataset using interleaved acquisition of both CLIP and CLAP HSQC), 5.3 h and 6.9 h respectively. For selected protons, traces along the proton dimension are shown. The decoupled spectra are shifted in the carbon dimension for easier comparison.

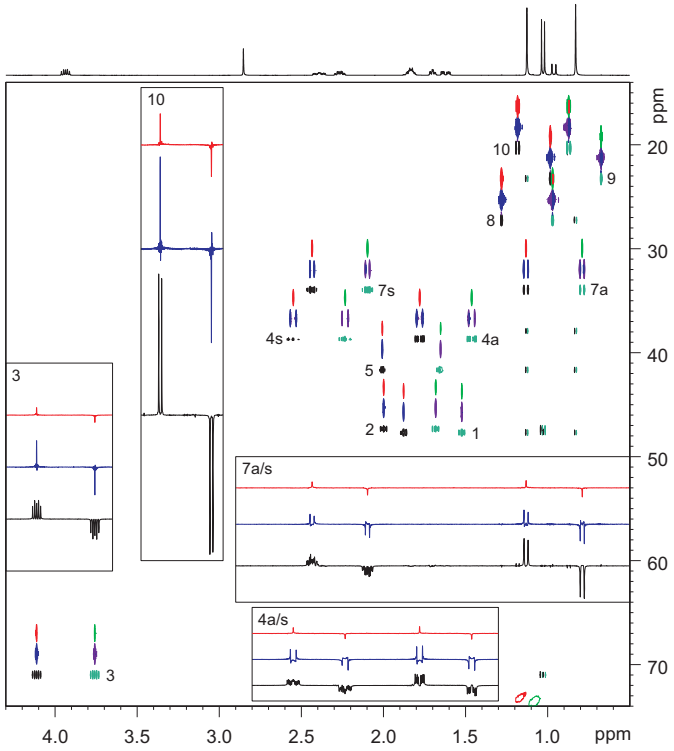

Figure S4: F_2-coupled CLAP HSQC spectra without homonuclear decoupling, with BIRD and with perfectBIRD homonuclear decoupling during acquisition, collected for (+)-IPC in isotropic CD_2Cl_2-solution at 9.4 T. The same color coding is used as in Figure S1. Experimental durations were 13.2 min (half duration of dataset using interleaved acquisition of both CLIP and CLAP HSQC), 5.3 h and 6.9 h respectively. For selected protons, traces along the proton dimension are shown. The decoupled spectra are shifted in the carbon dimension for easier comparison.

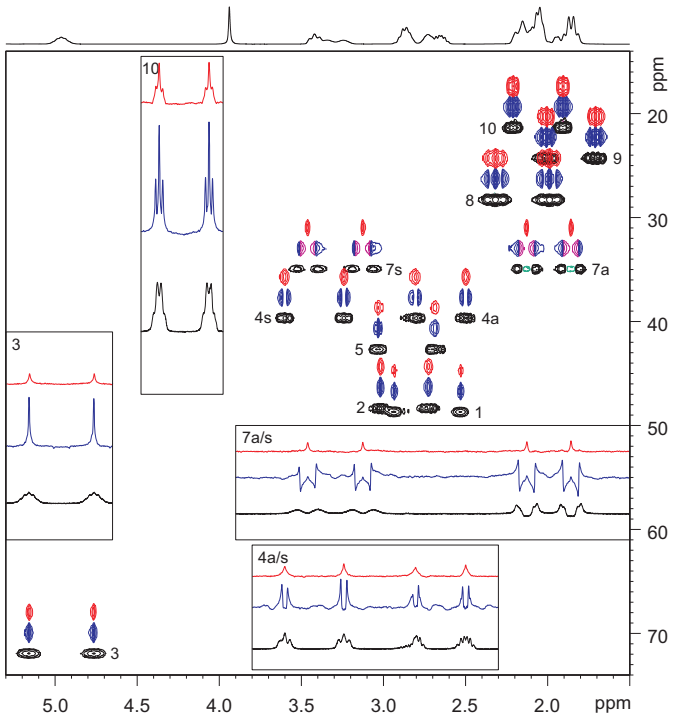

Figure S5: F_2-coupled CLIP HSQC spectra without homonuclear decoupling, with BIRD and with perfectBIRD homonuclear decoupling during acquisition, collected for (+)-IPC in anisotropic CD_2Cl_2/PBDG-solution at 9.4 T. The same color coding is used as in Figure S2. Experimental durations were 13.5 min (half duration of dataset using interleaved acquisition of both CLIP and CLAP HSQC), 2.9 h and 3.3 h respectively. For selected protons, traces along the proton dimension are shown. The decoupled spectra are shifted in the carbon dimension for easier comparison.

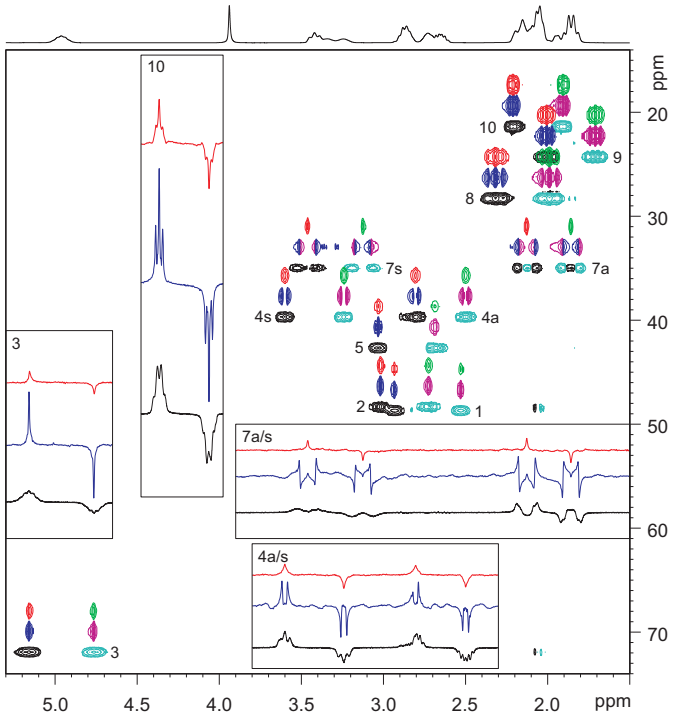

Figure S6: F_2-coupled CLAP HSQC spectra without homonuclear decoupling, with BIRD and with perfectBIRD homonuclear decoupling during acquisition, collected for (+)-IPC in anisotropic CD_2Cl_2/PBDG-solution at 9.4 T. Experimental durations were 13.2 min (half duration of dataset using interleaved acquisition of both CLIP and CLAP HSQC), 2.9 h and 3.3 h respectively. The same color coding is used as in Figure S1. For selected protons, traces along the proton dimension are shown. The decoupled spectra are shifted in the carbon dimension for easier comparison.

Coordinates for (+)-IPC

as previously used in Ref. [6].

```
29
plus_isopinocampheol
C10    -0.122      0.178     -0.118
H10a   -0.413      0.194      0.937
H10b   -1.040      0.194     -0.712
H10c    0.427      1.102     -0.322
C2      0.750     -1.046     -0.423
C3      1.326     -1.008     -1.865
H2      1.624     -0.986      0.236
C4      1.384     -2.392     -2.584
H3      0.701     -0.336     -2.464
O       2.628     -0.404     -1.761
C5      0.628     -3.500     -1.839
H4s     1.004     -2.290     -3.607
H4a     2.436     -2.687     -2.669
C7      1.123     -3.513     -0.369
H5      0.642     -4.439     -2.403
C1      0.073     -2.395     -0.114
H7s     0.913     -4.444      0.156
H7a     2.170     -3.246     -0.200
H1     -0.421     -2.366      0.864
H       2.955     -0.204     -2.647
C6     -0.761     -3.004     -1.306
C9     -1.631     -2.121     -2.205
C8     -1.638     -4.171     -0.825
H8a    -2.501     -3.797     -0.265
H8b    -2.024     -4.739     -1.678
H8c    -1.110     -4.874     -0.178
H9a    -2.017     -2.709     -3.046
H9b    -2.499     -1.741     -1.656
H9c    -1.112     -1.262     -2.627
```

Evaluation of the accuracy and precision of one-bond coupling constant extraction from BIRD and perfectBIRD decoupled spectra

In order to determine whether or not the modified HSQC experiments with homonuclear decoupling are suitable for one-bond coupling constant measurement, we evaluate here both the accuracy and the precision of the method.

First, we investigate a chloroform sample with slow transverse relaxation, representing a plain heteronuclear two spin-1/2 system. For this model system, an *accurate* and *precise* determination of $^1J_{CH}$ without interfering long-range couplings or signal overlap is possible from ^{13}C satellites observable in ordinary proton spectra. This allows us to evaluate the maximum achievable $^1J_{CH}$ measurement *accuracy* for different experiments, including the effects of instrumental imperfections.

Second, we return to the case of (+)-Isopinocampheol (IPC) to evaluate the *precision* achievable for coupling constant extraction in a more complex spin system, for both the isotropic and the weakly aligned sample. We discuss here the method of manual coupling constant extraction and confidence interval estimation employed, with a special emphasis on the different performances of the experiments compared in the main article.

Accuracy of one-bond coupling constant measurements in a two spin-1/2 system – experiments on $CHCl_3$

Results and discussion:

A total of 11 conventional proton spectra were used to determine the one-bond coupling constant for $CHCl_3$. These data were acquired interspersed with the more complex experiments being evaluated, in order to check reproducibility. No systematic change in the measured values was observed over the course of the measurements. Single scan spectra were sufficient to provide signal-to-noise ratios ranging from 700 to 900:1, depending on the quality of the shimming, for the ^{13}C satellites.

The signal separations extracted from these data scatter over a remarkably narrow range, with an average value of $^1J_{CH}(CHCl_3)$ = 209.122 Hz and a standard deviation of 0.001 Hz; however given the uncertainties of manual phasing we think that an uncertainty of 0.01 Hz is more appropriate for determining confidence limits. The absolute accuracy of this result should be tied through the instrument control software and hardware to the spectrometer crystal reference oscillator; typical units have frequency accuracies better than 1 in 10^6. (An alternative one-pulse experiment which allows the measurement of $^1J_{CH}$ is directly-observed proton coupled ^{13}C NMR with gated decoupling, but this offers much poorer sensitivity. From an experiment with a signal-to-noise ratio of 59:1 for the signal of interest, a value of $^1J_{CH}$ = (209.10 ± 0.05[a]) Hz was obtained.)

Having established a reference value for $^1J_{CH}$ in chloroform we now compare the results from different experiments used to determine one-bond coupling constants in Table S1. While we analyzed a set of 11 identically-measured proton spectra to determine the reference $^1J_{CH}$ value for $CHCl_3$, the values of $^1J_{CH}$ for the techniques described below were determined from single experiments, as is common practice in RDC analysis, and the confidence intervals were determined based on the shape of the signals used for extraction. The error ranges listed for these experiments are reported with a superscript "a", to highlight that these are confidence intervals determined according to the method described by Kummerlöwe *et al.*[3] to evaluate the uncertainty of the extraction procedure, as opposed to the standard deviations listed for the proton experiments. Both methods of error evaluation do not take into account possible systematic errors during the measurement.

All signal splittings reported here were determined both by manual extraction of the values (overlaying and shifting of 1D spectra or 1D traces from 2D spectra to achieve maximum overlap between the heteronuclear doublet components) and by Lorentzian deconvolution of the spectral regions of interest (deconvolution tool implemented in TopSpin 3.2, patchlevel 6; only one Lorentzian used for each satellite signal). The values obtained using the latter, which did not include signal phase as a parameter, are not reported here as for all spectra they deviated by less than 0.01 Hz from the values determined by manual extraction (peak positions are only reported to a precision of 0.01 Hz by the deconvolution tool used). The good agreement between the two methods of data extraction provides evidence that the precision of the coupling constant extraction is at least as good as this value. This, of course, is only true for well-resolved signals without homonuclear couplings, under good shimming conditions, and with sufficient signal-to-noise ratio.

F_1-coupled BIRD-scaled HSQC experiments can be regarded as a gold standard of $^1J_{CH}$ extraction precision for methine groups in systems with interfering long-range couplings, due to the decoupling of the latter in the dimension of coupling constant extraction[7]. Two experiments were performed for comparison, with differing sampling schemes in F_1 to achieve the required high digital resolution, employing either traditional sampling or non-uniform sampling. The results achieved with

this technique are in good agreement with the reference value from the proton experiments, demonstrating that these experiments also show excellent accuracy for this test system. The CLIP HSQC experiment without homonuclear decoupling also reproduced the value measured by the proton experiment very well. In a measurement with both proton and carbon transmitter on resonance and INEPT delays optimized for a one-bond coupling of 209 Hz, a signal separation of $^1J_{CH}$ = (209.12 ± 0.01[a]) Hz was obtained.

Both BIRD and perfectBIRD homodecoupled HSQC experiments provide slightly reduced measurement accuracy under the idealized conditions used, as compared to the ^{1}H and the CLIP HSQC experiment without homodecoupling. For perfectBIRD decoupled CLIP HSQC experiments, we tested the accuracy both under on resonance conditions and in experiments offsetting transmitter frequencies and setting INEPT and BIRD delays to a non-ideal value.

Table S1: Values for $^1J_{CH}$ in chloroform measured using different experimental methods.

experimental method	recovery delay [s]	transmitter offset [kHz]		INEPT/BIRD optimisation value [Hz]	measured $^1J_{CH}$ [Hz]
		^{1}H	^{13}C	= (4 d_1)$^{-1}$ = (2 d_3)$^{-1}$	
^{1}H (^{13}C satellites)	2	0			209.12 ± 0.01
^{13}C gated decoupled	2	0	0		209.10 ± 0.05[a]
F_1-coupled BIRD-scaled HSQC, traditional sampling	2	0	0	209	209.15 ± 0.04[a]
F_1-coupled BIRD-scaled HSQC, NUS (25%)	2	0	0	209	209.14 ± 0.08[a]
F_2-coupled CLIP HSQC	2	0	0	209	209.12 ± 0.01[a]
F_2-coupled CLIP HSQC BIRD decoupling	2	0	0	209	209.10 ± 0.01[a]
F_2-coupled CLIP HSQC BIRD decoupling	25	0	0	209	209.10 ± 0.02[a]
F_2-coupled CLIP HSQC perfectBIRD decoupling	2	0	0	209	209.08 ± 0.04[a]
F_2-coupled CLIP HSQC perfectBIRD decoupling	25	0	0	209	209.09 ± 0.06[a]
F_2-coupled CLIP HSQC perfectBIRD decoupling[1]	2	3.2	0	209	209.16 ± 0.04[a]
F_2-coupled CLIP HSQC perfectBIRD decoupling	2	0	6	209	209.08 ± 0.02[a]
F_2-coupled CLIP HSQC perfectBIRD decoupling	2	0	0	145	209.10 ± 0.03[a]

1: A first order phase correction was applied to the dataset prior to coupling constant extraction.

For F_2-coupled CLIP HSQC experiments with perfectBIRD decoupling, a very small systematic underestimation of the coupling constant with respect to the reference value for proton experiments was observed for all datasets except that acquired with the proton carrier frequency offset. We tentatively attribute this bias to uncertainty in manual phase correction for these particular experiments, which would lead to slight peak maximum displacements; these effects are under further investigation. Therefore we propose that, in addition to using the signal shape to estimate measurement uncertainty, the minimum uncertainty of the coupling constants determined with these methods should be assumed to include the effects of these systematic errors. Thus we suggest that for coupling constants extracted from CLIP/CLAP HSQC experiments acquired with BIRD or perfectBIRD homodecoupling, a lower bound error range of ± 0.05 Hz should be assumed, a range within which the data reported here show that the one-bond coupling measurement can be assumed to be accurate. This error should be combined with a suitable estimate for the coupling constant extraction precision. Throughout this work we assume that experimental inaccuracies are dominated by instrumental limitations and by the pulse sequences used, and that the same error range can be used for both isotropic and weakly aligned samples. A reduction of the accuracy of the measurements can be expected for signals showing second order effects.

Even though the experimental data shows that ± 0.05 Hz represents a realistic estimate of the systematic error for the parameter space we used in the experiments performed, when applying these to the measurement of RDCs the user is typically interested in a conservative estimate for the confidence interval to use. This is particularly true if decisions as to the rejection of structural models are to be made based on a very limited number of experimentally accessible values. In the following discussions, and in the main text, we therefore take the very conservative approach of using double the error range estimated ± 0.1 Hz, as the confidence interval within which we assume the results to be accurate. This confidence interval is then combined with the confidence interval of the coupling constant extraction precision, as evaluated according to the procedure of Kummerlöwe *et al.*[3], by Gaussian error propagation; again this is a very conservative approach, but one still costs very little. The errors thus obtained are listed in Tables S4 and S5, together with the coupling constants extracted. In the context of RDC analysis, the overall confidence interval will in most practical cases be dominated by the contribution of the extraction precision, rather than the measurement accuracy, as the extraction precision in aligned media even in favorable cases typically amounts to a few tenth of a Hertz.

Experimental settings and data extraction:

Experiments were performed on the 14.1 T system also used for the measurements described in the main text. A sample containing 75 µl $CHCl_3$ and 750 µl $CDCl_3$ without dopant was used. Experiments on the chloroform sample were performed at 300.9 K and using TopSpin 3.2 patchlevel 6.

For proton experiments, 64k complex data points were collected in the course of 6.55 s. An on resonance 90° hard pulse of 9.38 µs was used, followed by a receiver blanking delay of 6.5 µs. The relaxation delay was set to 2 s followed by a single scan. Data apodization with an exponentially decaying function with a rate constant of 0.1 Hz was applied.

For the gated decoupled ^{13}C experiment 2048 scans were averaged. 64k complex data points were collected during an acquisition period of 3.28 s. Both transmitter frequencies were set on resonance (77.196 ppm for ^{13}C and 7.285 ppm for ^{1}H). During the recovery delay of 2 s and the hard ^{13}C pulse of 13 µs length, 0.1 W waltz16 decoupling was applied to the proton channel. The splitting reported was extracted from a spectrum obtained after apodization of the time domain data with an exponentially decaying function with a rate constant of 0.1 Hz. Increasing the signal-to-noise ratio by the use of stronger apodization did not alter the result of the coupling constant extraction.

F_1-coupled BIRD-scaled HSQC experiments were collected using the pulse sequence reported in ref.[7c]. In the direct dimension 600 complex data points were collected during a 0.1 s acquisition period. In the indirect dimension, a spectral window of 6226 Hz was used and the data grid of 2k complex points was either fully sampled or sampled in a non-uniform way, collecting 512 complex points randomly distributed on this grid. In both cases the nominal FID resolution corresponds to 3 Hz. Both transmitter frequencies were set on resonance (77.196 ppm for ^{13}C and 7.285 ppm for ^{1}H). A two-step phase cycle was used, preceded by 16 dummy scans, with a recycle delay of 2 s. INEPT and BIRD delays were set to $(4*209\ Hz)^{-1}$ and $(2*209\ Hz)^{-1}$ respectively and a scaling factor of eight was used. Hard excitation pulses of 9.38 µs for protons and of 13 µs for carbon were used. For ^{13}C inversion during the INEPT elements, Chirp pulses (60 kHz sweep width, 500 µs duration, 20% smoothing) were used, while for ^{13}C refocusing 720-100-10 BIP (broad band inversion) pulses of 160 µs length were used. All gradients used a smoothed square shape (SMSQ10.100), were applied for 700 µs, and were followed by a 200 µs recovery delay. Gradients used 11 %, 11 %, 80 % and 20 % relative gradient amplitude.

For chloroform, F_2-coupled CLIP HSQC experiments were collected only for the first t_1 point ($t_1 = p_2+6\ \mu s = 24.76\ \mu s$; p_2 equals the length of the proton hard inversion pulse) and the resulting FID was processed to provide a 1D dataset, which was subsequently used for coupling constant extraction. In all cases four dummy scans and the full eight step phase cycle was used. Unless otherwise stated both transmitter frequencies were set on resonance with the signals of interest (77.196 ppm for ^{13}C and 7.285 ppm for ^{1}H). A recovery delay of 2 s was used and INEPT and BIRD delays were set to $d1 = d_2 = d_3/2 = (4*209\ Hz)^{-1}$. ^{1}H and ^{13}C 90° pulses of 9.38 µs and 13 µs length were used. With the exception of the final hard ^{13}C inversion pulse, Chirp pulses were used for ^{13}C inversion (60 kHz sweep width, 500 µs duration, 20% smoothing) and refocusing (four Chirp composite pulse with 60 kHz sweep width, 2 ms duration, 20% smoothing). The length of gradient pulses was shortened to 0.7 ms due to the reduced length of the INEPT steps. All gradient pulses used a smoothed square shape (SMSQ10.100) with an integration factor of 0.9 and were followed by a recovery delay of 200 µs. Relative gradients strengths used were $G_1 = 15$ %, $G_2 = 80$ %, $G_3 = 11$ %, $G_4 = 20.1$ %, $G_5 = 8$ %, $G_6 = 17$ % and $G_7 = 60$ %. CLIP HSQC experiments without homonuclear decoupling, as proposed by Luy *et al.*[2], only use G_2 and G_4.

The CLIP HSQC experiment without homodecoupling was acquired with 32k complex points and an acquisition duration of 3.28 s. In contrast to this, 128 chunks of 20 ms length were collected for homodecoupled CLIP HSQC experiments, providing an FID of 2.56 s length containing 25600 complex time points after data contraction. Prior to Fourier transformation the time domain signals were zero filled to 64k complex points and a decaying exponential apodization function (rate constant of 0.1 Hz) was applied. No first order phase correction was used unless otherwise stated.

In addition to systematic errors, the limitations of the extraction procedure itself should also be considered. Errors in the coupling constant extraction procedure can be caused by anti-phase contributions to the signals, by signal overlap, by insufficient signal-to-noise ratio, and by second order effects in the spectra. To evaluate whether or not the extraction procedure chosen allows the precise measurement of one-bond couplings and appropriate estimation of confidence intervals, we return to the case of (+)-IPC as a test system with interfering long-range couplings.

Throughout this paper we report values for one-bond coupling constants that were extracted by visual inspection of 1D traces that have been overlaid and shifted against each other, according to the procedure described in ref. [3]. This method is obviously biased by the operator performing the extraction. To illustrate that for a coupling constant extraction following this procedure the operator-dependent impact is within the confidence interval estimated, the extraction procedure was performed for the CLAP HSQC spectra shown in Figure 3 and Figure S1 by three different individuals (see Table S2 and S3). Comparison between the deviations observed and the error ranges listed in Table S5 shows that for the case studied, the operator-dependent influence is within the error ranges obtained. This holds true for all cases but $^{1}T_{C8H8}$ and $^{1}T_{C9H9}$, both extracted from the CLAP HSQC with perfectBIRD decoupling. The distorted line shape observed in perfectBIRD decoupled experiments for methyl groups of weakly aligned analytes thus seems to have an adverse effect on the coupling constant extraction precision for these groups.

A graphical comparison of the coupling constants and error ranges reported in Table S4 and S5 is provided in Figure S7. The confidence intervals for $^{1}J_{CH}$ values (isotropic sample) reported by the different techniques overlap for all protons. The comparison of the coupling constants measured under weak alignment of the analyte reveals a much stronger scattering of the data between the different methods. However using the above described method of error estimation, only three pairs of values not showing overlapping error ranges are obtained: The values for $^{1}T_{C9H9}$ measured with the CLAP HSQC experiment without homodecoupling and with perfectBIRD decoupling deviate outside the error margins, which might again be due to the distorted line shape observed for the methyl groups of aligned samples when using the perfectBIRD method. Further, the $^{1}T_{C1H1}$ extracted from the CLAP HSQC experiment without homodecoupling deviates from the corresponding values extracted from both the CLIP and the CLAP HSQC experiment with perfectBIRD decoupling. This deviation can be easily explained by the avoidance of partial signal cancellation due to signal overlap, observed in the CLAP HSQC without homodecoupling, through homodecoupling.

The major improvement we tried to achieve here for RDC analysis was an increase in precision of the coupling constant extraction for methylene protons. To illustrate the very convenient coupling constant extraction, even for weakly aligned samples, overlays of F_2 traces that have been shifted according to the coupling constants reported are shown in Figure S8.

Table S2: Coupling constants extracted by three different individuals from the spectra shown in Figure S1 ($^1J_{CH}$). Standard deviations are given for the different values determined.

		CLAP HSQC				BIRD CLAP HSQC				perfectBIRD CLAP HSQC			
C	H	$^1J_{CH}$ (Hz)			Standard deviation (Hz)	$^1J_{CH}$ (Hz)			Standard deviation (Hz)	$^1J_{CH}$ (Hz)			Standard deviation (Hz)
1	1	140.54	140.56	140.63	0.04	140.58	140.60	140.63	0.01	140.56	140.57	140.55	0.01
2	2	126.71	126.67	126.72	0.03	126.63	126.63	126.64	0.01	126.56	126.57	126.58	0.01
3	3	141.67	141.67	141.67	0.00	141.71	141.70	141.73	0.01	141.75	141.73	141.73	0.01
4	4s	126.37	126.32	126.33	0.03	126.32	126.35	126.37	0.01	126.31	126.31	126.32	0.01
4	4a	127.06	127.08	127.08	0.01	127.06	127.05	127.01	0.02	127.08	127.06	127.05	0.02
5	5	140.73	140.74	140.79	0.03	140.71	140.73	140.74	0.07	140.60	140.65	140.51	0.07
7	7s	134.85	134.80	134.98	0.09	134.84	134.85	134.87	0.02	134.78	134.77	134.75	0.02
7	7a	136.99	136.99	136.96	0.02	137.01	136.95	136.93	0.02	136.93	136.90	136.92	0.02
8	8	124.60	124.63	124.61	0.02	124.48	124.48	124.48	0.01	124.47	124.48	124.46	0.01
9	9	123.63	123.61	123.62	0.01	123.69	123.71	123.70	0.04	123.69	123.76	123.75	0.04
10	10	124.74	124.73	124.72	0.01	124.67	124.67	124.67	0.02	124.59	124.55	124.56	0.02

Table S3: Coupling constants extracted by three different individuals from the spectra shown in Figure 3 of the main text ($^1T_{CH}$). Standard deviations are given for the different values determined.

		CLAP HSQC				BIRD CLAP HSQC				perfectBIRD CLAP HSQC			
C	H	$^1T_{CH}$ (Hz)			Standard deviation (Hz)	$^1T_{CH}$ (Hz)			Standard deviation (Hz)	$^1T_{CH}$ (Hz)			Standard deviation (Hz)
1	1	162.66	163.21	164.25	0.81	160.67	160.42	160.61	0.13	160.47	160.45	160.33	0.08
2	2	117.25	117.25	116.11	0.66	116.92	116.93	116.93	0.01	116.71	116.66	116.52	0.10
3	3	158.30	158.16	158.11	0.10	158.40	158.38	158.40	0.01	158.56	158.87	159.04	0.24
4	4s	144.05	143.89	143.95	0.08	143.88	143.81	144.10	0.15	143.87	143.85	143.90	0.02
4	4a	122.48	122.61	122.52	0.07	122.60	122.66	122.65	0.03	122.60	122.66	122.72	0.06
5	5	138.35	138.50	138.66	0.15	137.44	137.45	137.44	0.01	137.15	136.94	136.58	0.29
7	7s	134.34	134.25	135.47	0.68	133.99	134.02	134.05	0.03	133.80	133.74	133.70	0.05
7	7a	106.96	106.81	107.28	0.24	106.94	106.96	107.11	0.09	106.78	106.64	106.81	0.09
8	8	131.99	131.76	131.70	0.15	131.90	131.97	132.02	0.06	131.75	131.81	131.44	0.20
9	9	118.38	118.56	118.63	0.13	118.79	118.78	118.98	0.11	118.95	119.00	119.65	0.39
10	10	121.34	121.15	121.09	0.13	121.10	121.05	121.00	0.05	120.80	120.72	120.36	0.24

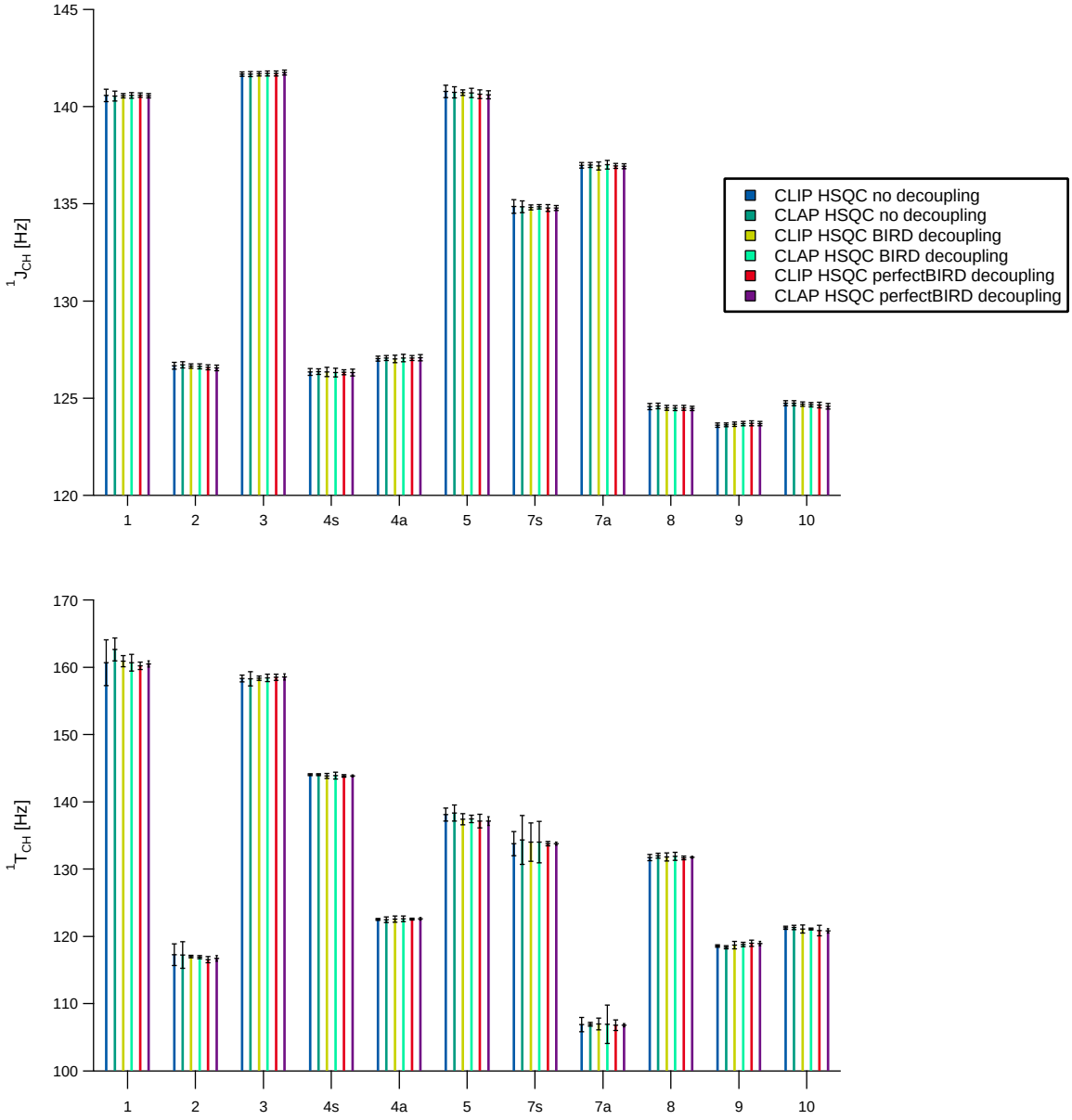

Figure S7: Scatter plots providing a graphical representation of the one-bond couplings measured for (+)-Isopinocampheol, as reported in Table S4 and S5. Scalar couplings measured for the isotropic CD_2Cl_2 sample are shown on the top, while total couplings determined for the analyte under weak alignment in PBDG/CD_2Cl_2 liquid crystalline phase are shown below.

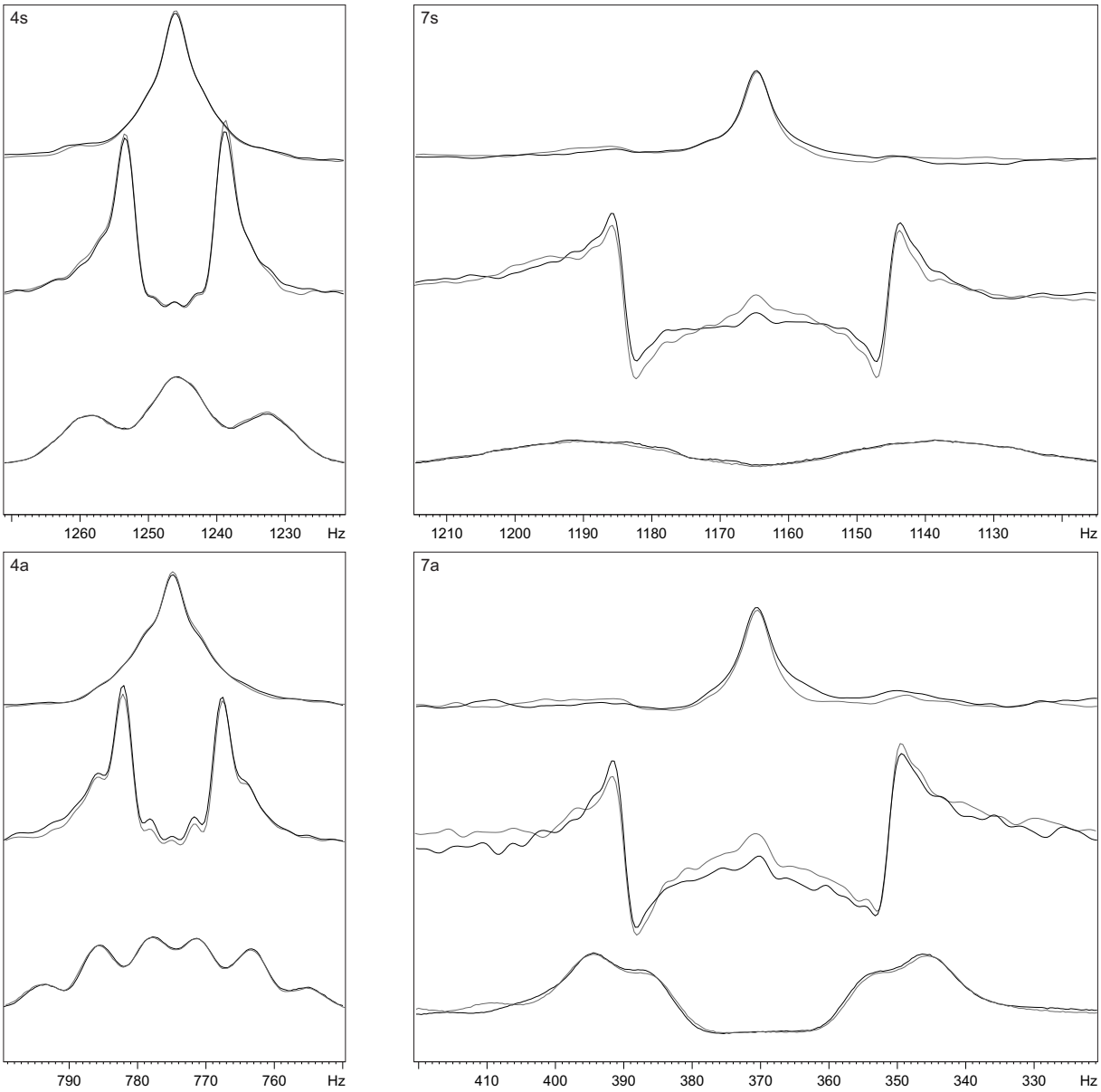

Figure S8: Overlays of the two components of the heteronuclear doublets observed for proton 4a, 4s, 7a and 7s of (+)-IPC weakly aligned in CD_2Cl_2/PBDG phase (9.05 %-wt; $\Delta\nu_Q$ = 107.6 Hz). The F_2 traces shown have been extracted from the CLIP HSQC spectra shown in Figure S2, which have been collected without homonuclear decoupling (bottom trace), with BIRD homonuclear decoupling (middle trace) and with perfectBIRD decoupling (top trace). The spectral regions containing the low field components are shown. The same spectra were duplicated, overlaid with the original ones and shifted by the corresponding $^1T_{CH}$ given in Table S4 and in Table 2 of the main article (shown in gray). All traces shown are normalized to the same noise level, as determined from an empty spectral region.

Coupling constants extracted from spectra collected at 600 MHz proton resonance frequency for (+)-Isopinocampheol

Table S4: Coupling constants extracted from the spectra shown in Figure 2 of the main text ($^1J_{CH}$) and in Figure S2 ($^1T_{CH}$). The method of confidence limit determination is described in the section "Evaluation of the accuracy and precision of one-bond coupling constant extraction from BIRD and perfectBIRD decoupled spectra"

		CLIP	BIRD CLIP	perfectBIRD CLIP	CLIP	BIRD CLIP	perfectBIRD CLIP	CLIP	BIRD CLIP	perfectBIRD CLIP
FID-res:		0.76 Hz	1.02 Hz	1.02 Hz	0.76 Hz	3.05 Hz	3.05 Hz			
C	H		$^1J_{CH}$ / Hz			$^1T_{CH}$ / Hz			$^1D_{CH}/^1D_{CC}$ / Hz	
1	1	140.57 ± 0.32	140.56 ± 0.11	140.59 ± 0.11	160.67 ± 3.42	160.92 ± 0.84	160.19 ± 0.54	10.05 ± 3.43	10.18 ± 0.85	9.80 ± 0.55
2	2	126.67 ± 0.17	126.65 ± 0.11	126.59 ± 0.12	117.27 ± 1.60	117.00 ± 0.19	116.53 ± 0.47	-4.70 ± 1.61	-4.83 ± 0.21	-5.03 ± 0.48
3	3	141.67 ± 0.11	141.69 ± 0.11	141.71 ± 0.12	158.31 ± 0.51	158.38 ± 0.33	158.51 ± 0.44	8.32 ± 0.52	8.35 ± 0.35	8.40 ± 0.45
4	4s	126.35 ± 0.18	126.35 ± 0.24	126.34 ± 0.13	144.03 ± 0.12	143.85 ± 0.37	143.83 ± 0.19	8.84 ± 0.21	8.75 ± 0.44	8.75 ± 0.23
4	4a	127.04 ± 0.12	127.02 ± 0.19	127.07 ± 0.13	122.54 ± 0.16	122.59 ± 0.44	122.56 ± 0.12	-2.25 ± 0.20	-2.22 ± 0.48	-2.26 ± 0.17
5	5	140.79 ± 0.32	140.72 ± 0.14	140.64 ± 0.23	138.10 ± 0.97	137.40 ± 0.82	137.12 ± 1.00	-1.35 ± 1.02	-1.66 ± 0.83	-1.76 ± 1.02
7	7s	134.87 ± 0.35	134.81 ± 0.13	134.79 ± 0.17	133.78 ± 1.77	134.03 ± 2.86	133.79 ± 0.32	-0.55 ± 1.80	-0.39 ± 2.86	-0.50 ± 0.36
7	7a	136.98 ± 0.15	136.94 ± 0.20	136.94 ± 0.12	106.89 ± 1.04	106.98 ± 0.86	106.81 ± 0.77	-15.05 ± 1.05	-14.98 ± 0.88	-15.07 ± 0.78
8	8	124.56 ± 0.16	124.51 ± 0.12	124.51 ± 0.12	131.70 ± 0.48	131.82 ± 0.59	131.66 ± 0.29	3.57 ± 0.50/-0.97 ± 0.50	3.65 ± 0.60/-0.99 ± 0.60	3.58 ± 0.31/-0.97 ± 0.31
9	9	123.61 ± 0.11	123.66 ± 0.11	123.70 ± 0.12	118.57 ± 0.19	118.71 ± 0.56	118.96 ± 0.47	-2.52 ± 0.21/0.69 ± 0.21	-2.48 ± 0.57/0.68 ± 0.57	-2.37 ± 0.48/0.65 ± 0.48
10	10	124.75 ± 0.13	124.69 ± 0.11	124.64 ± 0.15	121.28 ± 0.21	121.09 ± 0.60	120.87 ± 0.77	-1.74 ± 0.24/0.48 ± 0.24	-1.80 ± 0.61/0.49 ± 0.61	-1.89 ± 0.79/0.52 ± 0.79

Table S5: Coupling constants extracted from the spectra shown in Figure S1 ($^1J_{CH}$) and in Figure 3 of the main text ($^1T_{CH}$). The method of confidence limit determination is described in the section "Evaluation of the accuracy and precision of one-bond coupling constant extraction from BIRD and perfectBIRD decoupled spectra"

		CLAP	BIRD CLAP	perfectBIRD CLAP	CLAP	BIRD CLAP	perfectBIRD CLAP	CLAP	BIRD CLAP	perfectBIRD CLAP
FID-res:		0.76 Hz	1.02 Hz	1.02 Hz	0.76 Hz	3.05 Hz	3.05 Hz			
C	H		$^1J_{CH}$ / Hz			$^1T_{CH}$ / Hz			$^1D_{CH}/^1D_{CC}$ / Hz	
1	1	140.54 ± 0.26	140.58 ± 0.15	140.56 ± 0.11	162.66 ± 1.70	160.67 ± 1.22	160.47 ± 0.45	11.06 ± 1.72	10.05 ± 1.23	9.96 ± 0.46
2	2	126.71 ± 0.16	126.63 ± 0.12	126.56 ± 0.14	117.25 ± 1.97	116.92 ± 0.23	116.71 ± 0.43	-4.73 ± 1.97	-4.86 ± 0.26	-4.93 ± 0.45
3	3	141.67 ± 0.12	141.71 ± 0.12	141.75 ± 0.13	158.30 ± 1.08	158.40 ± 0.57	158.56 ± 0.46	8.32 ± 1.09	8.35 ± 0.59	8.41 ± 0.47
4	4s	126.37 ± 0.15	126.32 ± 0.22	126.31 ± 0.18	144.05 ± 0.12	143.88 ± 0.51	143.87 ± 0.15	8.84 ± 0.19	8.78 ± 0.56	8.78 ± 0.23
4	4a	127.06 ± 0.12	127.06 ± 0.19	127.08 ± 0.16	122.48 ± 0.40	122.60 ± 0.42	122.60 ± 0.17	-2.29 ± 0.41	-2.23 ± 0.45	-2.24 ± 0.23
5	5	140.73 ± 0.29	140.71 ± 0.24	140.60 ± 0.20	138.35 ± 1.19	137.44 ± 0.57	137.15 ± 0.65	-1.19 ± 1.22	-1.64 ± 0.62	-1.72 ± 0.68
7	7s	134.85 ± 0.31	134.84 ± 0.11	134.78 ± 0.13	134.34 ± 3.65	133.99 ± 3.08	133.80 ± 0.25	-0.25 ± 3.66	-0.42 ± 3.08	-0.49 ± 0.28
7	7a	136.99 ± 0.12	137.01 ± 0.22	136.93 ± 0.12	106.96 ± 0.29	106.94 ± 2.86	106.78 ± 0.23	-15.02 ± 0.32	-15.04 ± 2.86	-15.08 ± 0.25
8	8	124.60 ± 0.14	124.48 ± 0.12	124.47 ± 0.11	131.99 ± 0.37	131.90 ± 0.58	131.75 ± 0.15	3.70 ± 0.39/-1.01 ± 0.39	3.71 ± 0.59/-1.01 ± 0.59	3.64 ± 0.19/-0.99 ± 0.19
9	9	123.63 ± 0.10	123.69 ± 0.11	123.69 ± 0.11	118.38 ± 0.24	118.79 ± 0.33	118.95 ± 0.32	-2.63 ± 0.26/0.72 ± 0.26	-2.45 ± 0.35/0.67 ± 0.35	-2.37 ± 0.34/0.65 ± 0.34
10	10	124.74 ± 0.13	124.67 ± 0.11	124.59 ± 0.15	121.34 ± 0.30	121.10 ± 0.13	120.80 ± 0.33	-1.70 ± 0.33/0.47 ± 0.33	-1.79 ± 0.17/0.49 ± 0.17	-1.90 ± 0.36/0.52 ± 0.36

Quality factors

Table S6: Quality factors obtained by comparing the experimentally determined RDCs given in Table S4 and Table S5 with the values back-calculated for the structure given in the section "Coordinates for (+)-IPC".

	CLIP	BIRD-CLIP	perfectBIRD-CLIP	CLAP	BIRD-CLAP	perfectBIRD-CLAP
$Q^{[a]}$	0.023	0.023	0.020	0.047	0.021	0.020
$Q^{[b]}$	0.028	0.040	0.026	0.030	0.044	0.021
RMSD / Hz	0.159	0.155	0.139	0.322	0.142	0.139

[a]: as defined in[8], [b]: as defined in[9]

Signal overlap between C1-H1 and C2-H2 leads to partial signal cancellation in the CLAP HSQC spectra without homonuclear decoupling, affecting the coupling constant extracted for C1-H1. We mainly attribute the differences seen between the CLIP and the CLAP spectra without homonuclear decoupling to this effect. Signal narrowing circumvents this problem in the homodecoupled spectra. Addition/subtraction of the spectra according to the IPAP approach could be used to also circumvent this problem, even without homonuclear decoupling.

Comparison between experimental and back calculated RDCs

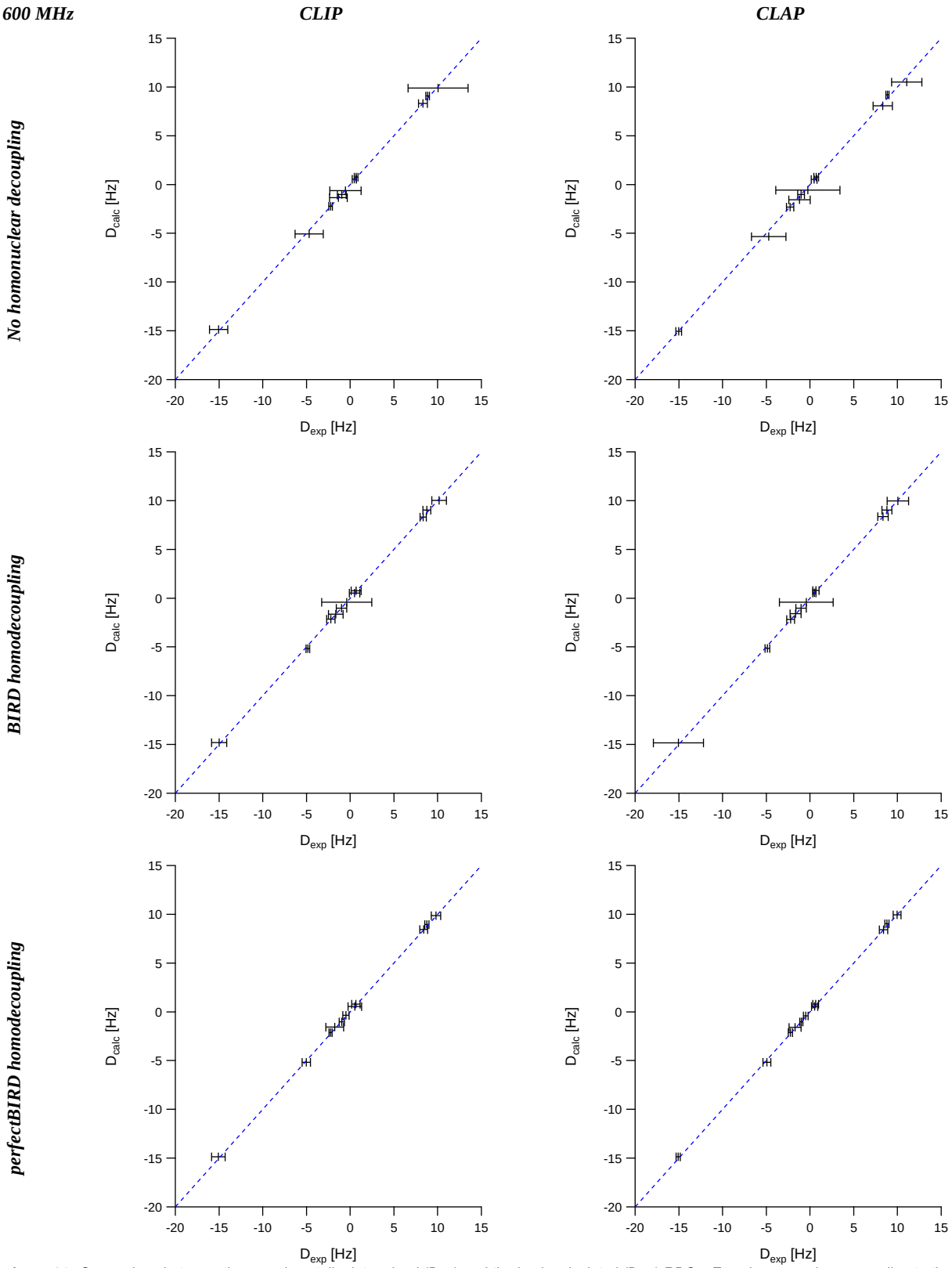

Figure S9: *Comparison between the experimentally determined (D_{exp}) and the back-calculated (D_{calc}) RDCs. Error bars are given according to the values listed in Table S4 and Table S5, though the experimentally assumed errors were not considered during the calculation of the alignment tensors.*

Output files generated by RDC@hotFCHT

F_2 coupled CLIP HSQC without homonuclear decoupling

```
Saupe vector: zz, xx-yy, xy, xz, yz
S_ij         :-5.271e-04  2.709e-04  5.155e-04  1.080e-04  1.328e-04

Averages and Error of Saupe vector
Losonczi Method, 1400 Monte-Carlo steps:  zz, xx-yy, xy, xz, yz
Average      :-5.245e-04  2.745e-04  5.164e-04  1.047e-04  1.311e-04
Error        : 7.089e-05  8.578e-05  3.841e-05  6.319e-05  4.384e-05
%-Error:     :    13.516     31.246      7.438     60.375     33.431
Atherton Method, from Sensitivities:  zz, xx-yy, xy, xz, yz
Error        : 3.490e-05  5.372e-05  4.105e-05  2.124e-05  3.135e-05
%-Error:     :     6.621     19.830      7.962     19.666     23.600

RDCs:
Atom1  Atom2          Dmax   RDCexp            RDCtheo           Residue  Weight
C1     H1       -22943.000   10.050 +- 3.430     9.898 +- 0.189    0.152    1.00
C2     H2       -22931.661   -4.700 +- 1.610    -5.063 +- 2.223    0.363    1.00
C3     H3       -22953.059    8.320 +- 0.520     8.304 +- 0.521    0.016    1.00
C4     H4s      -22943.802    8.840 +- 0.210     9.098 +- 2.129   -0.258    1.00
C4     H4a      -22954.664   -2.250 +- 0.200    -2.223 +- 0.593   -0.027    1.00
C5     H5       -22981.670   -1.350 +- 1.020    -1.355 +- 0.040    0.005    1.00
C7     H7s      -23375.805   -0.550 +- 1.800    -0.616 +- 1.769    0.066    1.00
C7     H7a      -23095.725  -15.050 +- 1.050   -14.867 +- 1.012   -0.183    1.00
C6     C8        -2092.574   -0.970 +- 0.500    -1.040 +- 0.096    0.070    1.00
C6     C9        -2116.163    0.690 +- 0.210     0.774 +- 0.025   -0.084    1.00
C2     C10       -2106.998    0.480 +- 0.240     0.549 +- 0.168   -0.069    1.00

Correlation of experimental and calculated RDCs:
RMSD /(Hz)   :    0.159
Q-Factor     :    0.023      (as defined by eg. Cornilescu)
Q-Da         :    0.006      (as given per default by PALES)
Q-Baltzar    :    0.028      (as defined by Baltzar Stevensson)
Chi^2        :    0.014      (RMSD normalized to the sum of all errors)
N over Chi^2 :  810.949      (Chi^2 normalized to the Number of RDCs (as used by Luy)
Pearson`s R  :    1.000      (Correlation Coefficient)
Pearson`s R2 :    0.999      (Correlation Coefficient squared)

Linear Fit of experimental and calculated RDCs:
Chi^2_Fit    :    0.142      (Residue of minimization)
Fit-Q        :    1.000      (Probability of real chi^2 higher than the one above)
Offset       :    0.057 +/-    0.153
Slope        :    0.999 +/-    0.059

Tensor properties:
Saupe Order Matrix:
 3.990e-04  5.155e-04  1.080e-04
 5.155e-04  1.281e-04  1.328e-04
 1.080e-04  1.328e-04 -5.271e-04

'Irreducible Representation' of Alignment Tensor:
   A0        A1R        A1I        A2R        A2I
-8.356e-04  1.398e-04  1.719e-04  1.753e-04  6.673e-04

General Magnitude of Alignment Tensor:
GMag         :  1.322e-03    (2*Da/DmaxPQ)*sqrt(pi*(4+3*R^2)/5) with DmaxPQ==1.0

Eigenvalues of SaupeMatrix (xx,yy,zz):
-2.642e-04 -5.531e-04  8.173e-04

Eigenvectors of SaupeMatrix (1st col xx, 2nd col yy, 3rd col zz):
-6.217e-01  1.313e-02 -7.831e-01
 7.716e-01  1.818e-01 -6.095e-01
 1.344e-01 -9.833e-01 -1.232e-01

Rotation of PAS to PDB frame (relative orientation):
Euler1 (ZYZ) :  alpha =  -82.219   beta =   97.074  gamma =  -37.895
Euler2 (ZYZ) :  alpha =   82.219   beta =   82.926  gamma =  142.105
Euler3 (ZYZ) :  alpha =  -97.781   beta =   82.926  gamma =  142.105
Euler4 (ZYZ) :  alpha =   97.781   beta =   97.074  gamma =  -37.895
Averages and Errors from Monte-Carlo-Simulation (1400 steps)
Average      :  alpha =  -79.952   beta =   96.759  gamma =  -37.792
Error        :  alpha =   12.890   beta =    2.340  gamma =    2.123
Cardan (XYZ) :    phi =  101.422  theta =  -51.548    psi = -178.790

Quaternion   : (x =    0.283; y =    0.694; z =   -0.574; w =    0.330)
Axis Angle   : (x =    0.300; y =    0.735; z =   -0.608; w =  141.402)

Da           :  4.086e-04    (Axial component of the Saupe tensor: 0.5*SaupeEigenValue(zz)

Dr           :  9.632e-05    (Rhombic component of the Saupe tensor: 1/3*(SaupeEigenValue(xx)-SaupeEigenValue(yy))

Aa           :  8.173e-04    (Axial component of the Alignment tensor: SaupeEigenValue(zz)

Ar           :  1.926e-04    (Rhombic component of the Alignment tensor: 2/3*(SaupeEigenValue(xx)-SaupeEigenValue(yy))

Da_NH        :  8.820e+00    (Da normalized to one-bond NH dipolar interaction: 0.5*21585.19*Aa)

R            :  2.357e-01    (Rhombicity of the Alignment tensor: Ar/Aa (range:[0,2/3]))

eta          :  3.536e-01    (Asymmetry parameter of the Alignment tensor: R/Rmax = (SaupeEigenValue(xx)-
SaupeEigenValue(yy))/SaupeEigenValue(zz) = (3/2)*R

GDO          :  8.341e-04    (Generalized degree of order: sqrt(2/3)*|SaupeEigenValues|)
```

F_2 coupled CLIP HSQC with BIRD decoupling

```
Saupe vector: zz, xx-yy, xy, xz, yz
S_ij         :-5.265e-04  2.622e-04  5.127e-04  1.154e-04  1.436e-04

Averages and Error of Saupe vector
Losonczi Method, 1300 Monte-Carlo steps:  zz, xx-yy, xy, xz, yz
Average      :-5.266e-04  2.598e-04  5.119e-04  1.155e-04  1.437e-04
Error        : 3.016e-05  6.401e-05  4.569e-05  1.830e-05  5.804e-05
%-Error:     :     5.727     24.642      8.925     15.843     40.404
Atherton Method, from Sensitivities:  zz, xx-yy, xy, xz, yz
Error        : 3.490e-05  5.372e-05  4.105e-05  2.124e-05  3.135e-05
%-Error:     :     6.628     20.486      8.007     18.415     21.834

RDCs:
Atom1  Atom2          Dmax   RDCexp            RDCtheo           Residue  Weight
C1     H1       -22943.000   10.180 +- 0.850    10.032 +- 0.329    0.148    1.00
C2     H2       -22931.661   -4.830 +- 0.210    -5.173 +- 1.075    0.343    1.00
C3     H3       -22953.059    8.350 +- 0.350     8.314 +- 1.438    0.036    1.00
C4     H4s      -22943.802    8.750 +- 0.440     9.028 +- 0.613   -0.278    1.00
C4     H4a      -22954.664   -2.220 +- 0.480    -2.151 +- 0.265   -0.069    1.00
C5     H5       -22981.670   -1.660 +- 0.830    -1.645 +- 0.538   -0.015    1.00
C7     H7s      -23375.805   -0.390 +- 2.860    -0.423 +- 1.471    0.033    1.00
C7     H7a      -23095.725  -14.980 +- 0.880   -14.813 +- 1.030   -0.167    1.00
C6     C8        -2092.574   -0.990 +- 0.600    -1.021 +- 0.028    0.031    1.00
C6     C9        -2116.163    0.680 +- 0.570     0.775 +- 0.120   -0.095    1.00
C2     C10       -2106.998    0.490 +- 0.610     0.537 +- 0.106   -0.047    1.00

Correlation of experimental and calculated RDCs:
RMSD /(Hz)   :    0.155
Q-Factor     :    0.023       (as defined by eg. Cornilescu)
Q-Da         :    0.006       (as given per default by PALES)
Q-Baltzar    :    0.040       (as defined by Baltzar Stevensson)
Chi^2        :    0.022       (RMSD normalized to the sum of all errors)
N over Chi^2 :  499.482       (Chi^2 normalized to the Number of RDCs (as used by Luy)
Pearson`s R  :    1.000       (Correlation Coefficient)
Pearson`s R2 :    0.999       (Correlation Coefficient squared)

Linear Fit of experimental and calculated RDCs:
Chi^2_Fit    :    0.295       (Residue of minimization)
Fit-Q        :    1.000       (Probability of real chi^2 higher than the one above)
Offset       :    0.035 +/-    0.241
Slope        :    1.004 +/-    0.048

Tensor properties:
Saupe Order Matrix:
 3.944e-04  5.127e-04  1.154e-04
 5.127e-04  1.321e-04  1.436e-04
 1.154e-04  1.436e-04 -5.265e-04

'Irreducible Representation' of Alignment Tensor:
   A0        A1R        A1I        A2R        A2I
-8.347e-04  1.493e-04  1.858e-04  1.697e-04  6.636e-04

General Magnitude of Alignment Tensor:
GMag         :  1.322e-03    (2*Da/DmaxPQ)*sqrt(pi*(4+3*R^2)/5) with DmaxPQ==1.0

Eigenvalues of SaupeMatrix (xx,yy,zz):
-2.598e-04 -5.566e-04  8.164e-04

Eigenvectors of SaupeMatrix (1st col xx, 2nd col yy, 3rd col zz):
-6.260e-01  1.464e-02 -7.797e-01
 7.668e-01  1.936e-01 -6.120e-01
 1.420e-01 -9.810e-01 -1.324e-01

Rotation of PAS to PDB frame (relative orientation):
Euler1 (ZYZ) :  alpha =  -81.764   beta =   97.609  gamma =  -38.128
Euler2 (ZYZ) :  alpha =   81.764   beta =   82.391  gamma =  141.872
Euler3 (ZYZ) :  alpha =  -98.236   beta =   82.391  gamma =  141.872
Euler4 (ZYZ) :  alpha =   98.236   beta =   97.609  gamma =  -38.128
Averages and Errors from Monte-Carlo-Simulation (1300 steps)
Average      :  alpha =  -82.456   beta =   97.623  gamma =  -38.195
Error        :  alpha =    8.160   beta =    2.013  gamma =    1.734
Cardan (XYZ) :    phi =  102.208  theta =  -51.233    psi = -178.660

Quaternion   : (x =    0.280; y =    0.699; z =   -0.570; w =    0.330)
Axis Angle   : (x =    0.296; y =    0.740; z =   -0.604; w =  141.481)

Da           :  4.082e-04    (Axial component of the Saupe tensor: 0.5*SaupeEigenValue(zz)

Dr           :  9.894e-05    (Rhombic component of the Saupe tensor: 1/3*(SaupeEigenValue(xx)-SaupeEigenValue(yy))

Aa           :  8.164e-04    (Axial component of the Alignment tensor: SaupeEigenValue(zz)

Ar           :  1.979e-04    (Rhombic component of the Alignment tensor: 2/3*(SaupeEigenValue(xx)-SaupeEigenValue(yy))

Da_NH        :  8.811e+00    (Da normalized to one-bond NH dipolar interaction: 0.5*21585.19*Aa)

R            :  2.424e-01    (Rhombicity of the Alignment tensor: Ar/Aa (range:[0,2/3]))

eta          :  3.636e-01    (Asymmetry parameter of the Alignment tensor: R/Rmax = (SaupeEigenValue(xx)-
SaupeEigenValue(yy))/SaupeEigenValue(zz) = (3/2)*R

GDO          :  8.342e-04    (Generalized degree of order: sqrt(2/3)*|SaupeEigenValues|)
```

F_2 coupled CLIP HSQC with perfectBIRD decoupling

```
Saupe vector: zz, xx-yy, xy, xz, yz
S_ij         :-5.205e-04  2.707e-04  5.167e-04  1.122e-04  1.441e-04

Averages and Error of Saupe vector
Losonczi Method, 1200 Monte-Carlo steps:  zz, xx-yy, xy, xz, yz
Average      :-5.208e-04  2.715e-04  5.167e-04  1.123e-04  1.449e-04
Error        : 1.552e-05  3.779e-05  2.241e-05  1.414e-05  2.315e-05
%-Error:     :     2.979     13.922      4.338     12.592     15.972
Atherton Method, from Sensitivities:  zz, xx-yy, xy, xz, yz
Error        : 3.490e-05  5.372e-05  4.105e-05  2.124e-05  3.135e-05
%-Error:     :     6.704     19.843      7.944     18.935     21.749

RDCs:
Atom1  Atom2          Dmax   RDCexp            RDCtheo           Residue  Weight
C1     H1       -22943.000    9.800 +- 0.550     9.859 +- 0.087   -0.059    1.00
C2     H2       -22931.661   -5.030 +- 0.480    -5.179 +- 0.680    0.149    1.00
C3     H3       -22953.059    8.400 +- 0.450     8.444 +- 0.554   -0.044    1.00
C4     H4s      -22943.802    8.750 +- 0.230     8.962 +- 0.420   -0.212    1.00
C4     H4a      -22954.664   -2.260 +- 0.170    -2.130 +- 0.099   -0.130    1.00
C5     H5       -22981.670   -1.760 +- 1.020    -1.569 +- 0.098   -0.191    1.00
C7     H7s      -23375.805   -0.500 +- 0.360    -0.367 +- 0.696   -0.133    1.00
C7     H7a      -23095.725  -15.070 +- 0.780   -14.855 +- 0.587   -0.215    1.00
C6     C8        -2092.574   -0.970 +- 0.310    -1.023 +- 0.014    0.053    1.00
C6     C9        -2116.163    0.650 +- 0.480     0.786 +- 0.044   -0.136    1.00
C2     C10       -2106.998    0.520 +- 0.790     0.551 +- 0.061   -0.031    1.00

Correlation of experimental and calculated RDCs:
RMSD /(Hz)   :    0.139
Q-Factor     :    0.020       (as defined by eg. Cornilescu)
Q-Da         :    0.006       (as given per default by PALES)
Q-Baltzar    :    0.026       (as defined by Baltzar Stevensson)
Chi^2        :    0.060       (RMSD normalized to the sum of all errors)
N over Chi^2 :  183.947       (Chi^2 normalized to the Number of RDCs (as used by Luy)
Pearson`s R  :    1.000       (Correlation Coefficient)
Pearson`s R2 :    1.000       (Correlation Coefficient squared)

Linear Fit of experimental and calculated RDCs:
Chi^2_Fit    :    0.449       (Residue of minimization)
Fit-Q        :    1.000       (Probability of real chi^2 higher than the one above)
Offset       :    0.089 +/-    0.133
Slope        :    1.002 +/-    0.029

Tensor properties:
Saupe Order Matrix:
 3.956e-04  5.167e-04  1.122e-04
 5.167e-04  1.249e-04  1.441e-04
 1.122e-04  1.441e-04 -5.205e-04

'Irreducible Representation' of Alignment Tensor:
   A0        A1R        A1I        A2R        A2I
-8.252e-04  1.452e-04  1.866e-04  1.752e-04  6.688e-04

General Magnitude of Alignment Tensor:
GMag         :  1.322e-03    (2*Da/DmaxPQ)*sqrt(pi*(4+3*R^2)/5) with DmaxPQ==1.0

Eigenvalues of SaupeMatrix (xx,yy,zz):
-2.665e-04 -5.513e-04  8.178e-04

Eigenvectors of SaupeMatrix (1st col xx, 2nd col yy, 3rd col zz):
-6.239e-01  3.654e-03 -7.815e-01
 7.652e-01  2.058e-01 -6.100e-01
 1.586e-01 -9.786e-01 -1.312e-01

Rotation of PAS to PDB frame (relative orientation):
Euler1 (ZYZ) :  alpha =  -80.794   beta =   97.539  gamma =  -37.976
Euler2 (ZYZ) :  alpha =   80.794   beta =   82.461  gamma =  142.024
Euler3 (ZYZ) :  alpha =  -99.206   beta =   82.461  gamma =  142.024
Euler4 (ZYZ) :  alpha =   99.206   beta =   97.539  gamma =  -37.976
Averages and Errors from Monte-Carlo-Simulation (1200 steps)
Average      :  alpha =  -80.785   beta =   97.560  gamma =  -37.988
Error        :  alpha =    2.978   beta =    0.898  gamma =    0.923
Cardan (XYZ) :    phi =  102.139  theta =  -51.394    psi = -179.664

Quaternion   : (x =    0.275; y =    0.700; z =   -0.567; w =    0.336)
Axis Angle   : (x =    0.291; y =    0.743; z =   -0.602; w =  140.776)

Da           :  4.089e-04    (Axial component of the Saupe tensor: 0.5*SaupeEigenValue(zz)

Dr           :  9.492e-05    (Rhombic component of the Saupe tensor: 1/3*(SaupeEigenValue(xx)-SaupeEigenValue(yy))

Aa           :  8.178e-04    (Axial component of the Alignment tensor: SaupeEigenValue(zz)

Ar           :  1.898e-04    (Rhombic component of the Alignment tensor: 2/3*(SaupeEigenValue(xx)-SaupeEigenValue(yy))

Da_NH        :  8.826e+00    (Da normalized to one-bond NH dipolar interaction: 0.5*21585.19*Aa)

R            :  2.321e-01    (Rhombicity of the Alignment tensor: Ar/Aa (range:[0,2/3]))

eta          :  3.482e-01    (Asymmetry parameter of the Alignment tensor: R/Rmax = (SaupeEigenValue(xx)-
SaupeEigenValue(yy))/SaupeEigenValue(zz) = (3/2)*R

GDO          :  8.342e-04    (Generalized degree of order: sqrt(2/3)*|SaupeEigenValues|)
```

F_2 coupled CLAP HSQC without homonuclear decoupling

```
Saupe vector: zz, xx-yy, xy, xz, yz
S_ij         :-5.446e-04  2.619e-04  5.128e-04  1.245e-04  1.368e-04

Averages and Error of Saupe vector
Losonczi Method, 1200 Monte-Carlo steps:  zz, xx-yy, xy, xz, yz
Average      :-5.424e-04  2.655e-04  5.106e-04  1.243e-04  1.404e-04
Error        : 4.518e-05  8.908e-05  6.304e-05  4.519e-05  8.073e-05
%-Error:     :     8.331     33.556     12.344     36.339     57.516
Atherton Method, from Sensitivities:  zz, xx-yy, xy, xz, yz
Error        : 3.490e-05  5.372e-05  4.105e-05  2.124e-05  3.135e-05
%-Error:     :     6.409     20.511      8.004     17.066     22.907

RDCs:
Atom1  Atom2          Dmax   RDCexp            RDCtheo           Residue  Weight
C1     H1       -22943.000   11.060 +- 1.720    10.495 +- 0.146    0.565    1.00
C2     H2       -22931.661   -4.730 +- 1.970    -5.344 +- 1.931    0.614    1.00
C3     H3       -22953.059    8.320 +- 1.090     8.061 +- 1.713    0.259    1.00
C4     H4s      -22943.802    8.840 +- 0.190     9.201 +- 1.206   -0.361    1.00
C4     H4a      -22954.664   -2.290 +- 0.410    -2.311 +- 0.466    0.021    1.00
C5     H5       -22981.670   -1.190 +- 1.220    -1.551 +- 0.734    0.361    1.00
C7     H7s      -23375.805   -0.250 +- 3.660    -0.581 +- 2.147    0.331    1.00
C7     H7a      -23095.725  -15.020 +- 0.320   -15.056 +- 1.527    0.036    1.00
C6     C8        -2092.574   -1.010 +- 0.390    -1.034 +- 0.057    0.024    1.00
C6     C9        -2116.163    0.720 +- 0.260     0.754 +- 0.139   -0.034    1.00
C2     C10       -2106.998    0.470 +- 0.330     0.530 +- 0.159   -0.060    1.00

Correlation of experimental and calculated RDCs:
RMSD /(Hz)   :    0.322
Q-Factor     :    0.047      (as defined by eg. Cornilescu)
Q-Da         :    0.013      (as given per default by PALES)
Q-Baltzar    :    0.030      (as defined by Baltzar Stevensson)
Chi^2        :    0.048      (RMSD normalized to the sum of all errors)
N over Chi^2 :  227.380      (Chi^2 normalized to the Number of RDCs (as used by Luy)
Pearson`s R  :    0.999      (Correlation Coefficient)
Pearson`s R2 :    0.998      (Correlation Coefficient squared)

Linear Fit of experimental and calculated RDCs:
Chi^2_Fit    :    0.365      (Residue of minimization)
Fit-Q        :    1.000      (Probability of real chi^2 higher than the one above)
Offset       :    0.010 +/-    0.182
Slope        :    1.006 +/-    0.066

Tensor properties:
Saupe Order Matrix:
 4.032e-04  5.128e-04  1.245e-04
 5.128e-04  1.413e-04  1.368e-04
 1.245e-04  1.368e-04 -5.446e-04

'Irreducible Representation' of Alignment Tensor:
   A0        A1R        A1I        A2R        A2I
-8.633e-04  1.611e-04  1.771e-04  1.695e-04  6.638e-04

General Magnitude of Alignment Tensor:
GMag         :  1.341e-03    (2*Da/DmaxPQ)*sqrt(pi*(4+3*R^2)/5) with DmaxPQ==1.0

Eigenvalues of SaupeMatrix (xx,yy,zz):
-2.539e-04 -5.719e-04  8.258e-04

Eigenvectors of SaupeMatrix (1st col xx, 2nd col yy, 3rd col zz):
-6.237e-01  4.243e-02 -7.805e-01
 7.755e-01  1.587e-01 -6.111e-01
 9.797e-02 -9.864e-01 -1.319e-01

Rotation of PAS to PDB frame (relative orientation):
Euler1 (ZYZ) :  alpha =  -84.328   beta =   97.581  gamma =  -38.061
Euler2 (ZYZ) :  alpha =   84.328   beta =   82.419  gamma =  141.939
Euler3 (ZYZ) :  alpha =  -95.672   beta =   82.419  gamma =  141.939
Euler4 (ZYZ) :  alpha =   95.672   beta =   97.581  gamma =  -38.061
Averages and Errors from Monte-Carlo-Simulation (1200 steps)
Average      :  alpha =  -84.213   beta =   97.640  gamma =  -37.956
Error        :  alpha =   11.166   beta =    2.961  gamma =    2.467
Cardan (XYZ) :    phi =  102.181  theta =  -51.304    psi = -176.108

Quaternion   : (x =    0.296; y =    0.692; z =   -0.577; w =    0.317)
Axis Angle   : (x =    0.312; y =    0.730; z =   -0.609; w =  142.983)

Da           :  4.129e-04    (Axial component of the Saupe tensor: 0.5*SaupeEigenValue(zz)

Dr           :  1.060e-04    (Rhombic component of the Saupe tensor: 1/3*(SaupeEigenValue(xx)-SaupeEigenValue(yy))

Aa           :  8.258e-04    (Axial component of the Alignment tensor: SaupeEigenValue(zz)

Ar           :  2.120e-04    (Rhombic component of the Alignment tensor: 2/3*(SaupeEigenValue(xx)-SaupeEigenValue(yy))

Da_NH        :  8.913e+00    (Da normalized to one-bond NH dipolar interaction: 0.5*21585.19*Aa)

R            :  2.568e-01    (Rhombicity of the Alignment tensor: Ar/Aa (range:[0,2/3]))

eta          :  3.851e-01    (Asymmetry parameter of the Alignment tensor: R/Rmax = (SaupeEigenValue(xx)-
SaupeEigenValue(yy))/SaupeEigenValue(zz) = (3/2)*R

GDO          :  8.460e-04    (Generalized degree of order: sqrt(2/3)*|SaupeEigenValues|)
```

F_2 coupled CLAP HSQC with BIRD decoupling

```
Saupe vector: zz, xx-yy, xy, xz, yz
S_ij         :-5.253e-04  2.667e-04  5.142e-04  1.132e-04  1.424e-04

Averages and Error of Saupe vector
Losonczi Method, 1200 Monte-Carlo steps:  zz, xx-yy, xy, xz, yz
Average      :-5.270e-04  2.656e-04  5.134e-04  1.142e-04  1.415e-04
Error        : 4.342e-05  9.424e-05  7.462e-05  2.466e-05  6.328e-05
%-Error:     :     8.239     35.478     14.534     21.592     44.707
Atherton Method, from Sensitivities:  zz, xx-yy, xy, xz, yz
Error        : 3.490e-05  5.372e-05  4.105e-05  2.124e-05  3.135e-05
%-Error:     :     6.644     20.143      7.982     18.758     22.012

RDCs:
Atom1  Atom2          Dmax   RDCexp            RDCtheo           Residue  Weight
C1     H1       -22943.000   10.050 +- 1.230     9.965 +- 0.483    0.085    1.00
C2     H2       -22931.661   -4.860 +- 0.260    -5.161 +- 1.512    0.301    1.00
C3     H3       -22953.059    8.350 +- 0.590     8.356 +- 1.925   -0.006    1.00
C4     H4s      -22943.802    8.780 +- 0.560     9.029 +- 0.928   -0.249    1.00
C4     H4a      -22954.664   -2.230 +- 0.450    -2.168 +- 0.480   -0.062    1.00
C5     H5       -22981.670   -1.640 +- 0.620    -1.580 +- 0.341   -0.060    1.00
C7     H7s      -23375.805   -0.420 +- 3.080    -0.426 +- 1.669    0.006    1.00
C7     H7a      -23095.725  -15.040 +- 2.860   -14.845 +- 1.551   -0.195    1.00
C6     C8        -2092.574   -1.010 +- 0.590    -1.024 +- 0.003    0.014    1.00
C6     C9        -2116.163    0.670 +- 0.350     0.779 +- 0.159   -0.109    1.00
C2     C10       -2106.998    0.490 +- 0.170     0.543 +- 0.184   -0.053    1.00

Correlation of experimental and calculated RDCs:
RMSD /(Hz)   :    0.142
Q-Factor     :    0.021      (as defined by eg. Cornilescu)
Q-Da         :    0.006      (as given per default by PALES)
Q-Baltzar    :    0.044      (as defined by Baltzar Stevensson)
Chi^2        :    0.011      (RMSD normalized to the sum of all errors)
N over Chi^2 : 1047.209      (Chi^2 normalized to the Number of RDCs (as used by Luy)
Pearson`s R  :    1.000      (Correlation Coefficient)
Pearson`s R2 :    1.000      (Correlation Coefficient squared)

Linear Fit of experimental and calculated RDCs:
Chi^2_Fit    :    0.122      (Residue of minimization)
Fit-Q        :    1.000      (Probability of real chi^2 higher than the one above)
Offset       :    0.055 +/-    0.179
Slope        :    1.008 +/-    0.073

Tensor properties:
Saupe Order Matrix:
 3.960e-04  5.142e-04  1.132e-04
 5.142e-04  1.293e-04  1.424e-04
 1.132e-04  1.424e-04 -5.253e-04

'Irreducible Representation' of Alignment Tensor:
   A0        A1R        A1I        A2R        A2I
-8.328e-04  1.466e-04  1.843e-04  1.726e-04  6.656e-04

General Magnitude of Alignment Tensor:
GMag         :  1.323e-03    (2*Da/DmaxPQ)*sqrt(pi*(4+3*R^2)/5) with DmaxPQ==1.0

Eigenvalues of SaupeMatrix (xx,yy,zz):
-2.622e-04 -5.550e-04  8.172e-04

Eigenvectors of SaupeMatrix (1st col xx, 2nd col yy, 3rd col zz):
-6.245e-01  1.082e-02 -7.809e-01
 7.671e-01  1.959e-01 -6.108e-01
 1.464e-01 -9.806e-01 -1.307e-01

Rotation of PAS to PDB frame (relative orientation):
Euler1 (ZYZ) :  alpha =  -81.509   beta =   97.508  gamma =  -38.032
Euler2 (ZYZ) :  alpha =   81.509   beta =   82.492  gamma =  141.968
Euler3 (ZYZ) :  alpha =  -98.491   beta =   82.492  gamma =  141.968
Euler4 (ZYZ) :  alpha =   98.491   beta =   97.508  gamma =  -38.032
Averages and Errors from Monte-Carlo-Simulation (1200 steps)
Average      :  alpha =  -82.468   beta =   97.533  gamma =  -38.172
Error        :  alpha =    9.406   beta =    2.271  gamma =    2.170
Cardan (XYZ) :    phi =  102.075  theta =  -51.344    psi = -179.007

Quaternion   : (x =    0.278; y =    0.698; z =   -0.570; w =    0.332)
Axis Angle   : (x =    0.295; y =    0.740; z =   -0.604; w =  141.228)

Da           :  4.086e-04    (Axial component of the Saupe tensor: 0.5*SaupeEigenValue(zz)

Dr           :  9.761e-05    (Rhombic component of the Saupe tensor: 1/3*(SaupeEigenValue(xx)-SaupeEigenValue(yy))

Aa           :  8.172e-04    (Axial component of the Alignment tensor: SaupeEigenValue(zz)

Ar           :  1.952e-04    (Rhombic component of the Alignment tensor: 2/3*(SaupeEigenValue(xx)-SaupeEigenValue(yy))

Da_NH        :  8.820e+00    (Da normalized to one-bond NH dipolar interaction: 0.5*21585.19*Aa)

R            :  2.389e-01    (Rhombicity of the Alignment tensor: Ar/Aa (range:[0,2/3]))

eta          :  3.583e-01    (Asymmetry parameter of the Alignment tensor: R/Rmax = (SaupeEigenValue(xx)-
SaupeEigenValue(yy))/SaupeEigenValue(zz) = (3/2)*R

GDO          :  8.345e-04    (Generalized degree of order: sqrt(2/3)*|SaupeEigenValues|)
```

F_2 coupled CLIP HSQC with perfectBIRD decoupling

```
Saupe vector: zz, xx-yy, xy, xz, yz
S_ij         :-5.243e-04  2.675e-04  5.172e-04  1.128e-04  1.434e-04

Averages and Error of Saupe vector
Losonczi Method, 1200 Monte-Carlo steps:  zz, xx-yy, xy, xz, yz
Average      :-5.244e-04  2.670e-04  5.170e-04  1.125e-04  1.434e-04
Error        : 1.204e-05  2.475e-05  1.565e-05  1.229e-05  1.657e-05
%-Error:     :     2.297      9.270      3.027     10.919     11.558
Atherton Method, from Sensitivities:  zz, xx-yy, xy, xz, yz
Error        : 3.490e-05  5.372e-05  4.105e-05  2.124e-05  3.135e-05
%-Error:     :     6.656     20.083      7.936     18.833     21.853

RDCs:
Atom1  Atom2          Dmax   RDCexp            RDCtheo           Residue  Weight
C1     H1       -22943.000    9.960 +- 0.460    9.940 +- 0.032    0.020    1.00
C2     H2       -22931.661   -4.930 +- 0.450   -5.166 +- 0.518    0.236    1.00
C3     H3       -22953.059    8.410 +- 0.470    8.428 +- 0.359   -0.018    1.00
C4     H4s      -22943.802    8.780 +- 0.230    9.025 +- 0.348   -0.245    1.00
C4     H4a      -22954.664   -2.240 +- 0.230   -2.132 +- 0.106   -0.108    1.00
C5     H5       -22981.670   -1.720 +- 0.680   -1.591 +- 0.087   -0.129    1.00
C7     H7s      -23375.805   -0.490 +- 0.280   -0.422 +- 0.495   -0.068    1.00
C7     H7a      -23095.725  -15.080 +- 0.250  -14.873 +- 0.398   -0.207    1.00
C6     C8        -2092.574   -0.990 +- 0.190   -1.028 +- 0.013    0.038    1.00
C6     C9        -2116.163    0.650 +- 0.340    0.785 +- 0.028   -0.135    1.00
C2     C10       -2106.998    0.520 +- 0.360    0.549 +- 0.044   -0.029    1.00

Correlation of experimental and calculated RDCs:
RMSD /(Hz)   :    0.139
Q-Factor     :    0.020       (as defined by eg. Cornilescu)
Q-Da         :    0.006       (as given per default by PALES)
Q-Baltzar    :    0.021       (as defined by Baltzar Stevensson)
Chi^2        :    0.131       (RMSD normalized to the sum of all errors)
N over Chi^2 :   84.032       (Chi^2 normalized to the Number of RDCs (as used by Luy)
Pearson`s R  :    1.000       (Correlation Coefficient)
Pearson`s R2 :    1.000       (Correlation Coefficient squared)

Linear Fit of experimental and calculated RDCs:
Chi^2_Fit    :    0.876       (Residue of minimization)
Fit-Q        :    1.000       (Probability of real chi^2 higher than the one above)
Offset       :    0.051 +/-    0.109
Slope        :    1.000 +/-    0.021

Tensor properties:
Saupe Order Matrix:
 3.959e-04  5.172e-04  1.128e-04
 5.172e-04  1.284e-04  1.434e-04
 1.128e-04  1.434e-04 -5.243e-04

'Irreducible Representation' of Alignment Tensor:
   A0        A1R        A1I        A2R        A2I
-8.313e-04  1.460e-04  1.857e-04  1.731e-04  6.695e-04

General Magnitude of Alignment Tensor:
GMag         :  1.326e-03    (2*Da/DmaxPQ)*sqrt(pi*(4+3*R^2)/5) with DmaxPQ==1.0

Eigenvalues of SaupeMatrix (xx,yy,zz):
-2.652e-04 -5.545e-04  8.197e-04

Eigenvectors of SaupeMatrix (1st col xx, 2nd col yy, 3rd col zz):
-6.249e-01  7.299e-03 -7.806e-01
 7.658e-01  2.003e-01 -6.112e-01
 1.519e-01 -9.797e-01 -1.307e-01

Rotation of PAS to PDB frame (relative orientation):
Euler1 (ZYZ) :  alpha =  -81.189   beta =   97.512  gamma =  -38.058
Euler2 (ZYZ) :  alpha =   81.189   beta =   82.488  gamma =  141.942
Euler3 (ZYZ) :  alpha =  -98.811   beta =   82.488  gamma =  141.942
Euler4 (ZYZ) :  alpha =   98.811   beta =   97.512  gamma =  -38.058
Averages and Errors from Monte-Carlo-Simulation (1200 steps)
Average      :  alpha =  -81.185   beta =   97.502  gamma =  -38.073
Error        :  alpha =    2.544   beta =    0.652  gamma =    0.644
Cardan (XYZ) :    phi =  102.075  theta =  -51.319    psi = -179.331

Quaternion   : (x =    0.276; y =    0.699; z =   -0.569; w =    0.333)
Axis Angle   : (x =    0.293; y =    0.742; z =   -0.603; w =  141.052)

Da           :  4.099e-04    (Axial component of the Saupe tensor: 0.5*SaupeEigenValue(zz)

Dr           :  9.642e-05    (Rhombic component of the Saupe tensor: 1/3*(SaupeEigenValue(xx)-SaupeEigenValue(yy))

Aa           :  8.197e-04    (Axial component of the Alignment tensor: SaupeEigenValue(zz)

Ar           :  1.928e-04    (Rhombic component of the Alignment tensor: 2/3*(SaupeEigenValue(xx)-SaupeEigenValue(yy))

Da_NH        :  8.847e+00    (Da normalized to one-bond NH dipolar interaction: 0.5*21585.19*Aa)

R            :  2.352e-01    (Rhombicity of the Alignment tensor: Ar/Aa (range:[0,2/3]))

eta          :  3.529e-01    (Asymmetry parameter of the Alignment tensor: R/Rmax = (SaupeEigenValue(xx)-
SaupeEigenValue(yy))/SaupeEigenValue(zz) = (3/2)*R

GDO          :  8.366e-04    (Generalized degree of order: sqrt(2/3)*|SaupeEigenValues|)
```

Signal appearance in the case of strongly coupled spin systems

As mentioned in the main article, full refocusing of strong coupling evolution cannot be achieved by the homonuclear decoupling schemes used throughout this paper. To the best of our knowledge, no method of homonuclear broadband decoupling has been presented so far that is able to suppress fully the effects of strong coupling, although some recent results with the PSYCHE method show promise[10]. Particularly in the case of coupling constant extraction, the possibility to identify strongly coupled signals is of prime importance, as strong coupling is known to interfere with the extraction procedure, unless specialized approaches are used[11]. In this section we therefore illustrate the effect of strong coupling interference for the case of (-)-menthol in isotropic solution. A very similar comparison has also been made in the work by Reinsperger and Luy to illustrate this effect for the CLIP-RESET (different terminology for the F_2 BIRD decoupled CLIP HSQC experiment discussed herei) and CT-CLIP-RESET experiments[12].

Figure S10 compares CLIP HSQC spectra of (-)-menthol acquired with homonuclear BIRD and perfectBIRD decoupling in the proton dimension with a CLIP HSQC spectrum obtained without homodecoupling. For some of the signals, such as those for positions 2 and 4', it is already visible in this representation that the heteronuclear doublet pattern provides different signal intensities for the two doublet components, which should be taken as a first indication of strong coupling effects. However a much easier discrimination of strong coupling effects can be performed, when examining F_2 traces extracted from the spectra, as shown in Figure S11. Signals from weakly coupled protons appear as sharp signals, with similar signal shape and intensity for both doublet components, providing an easy way to determine signal separations by overlaying both components of the heteronuclear doublet. This holds true for methyl groups (e.g.: protons 8), methylene groups (e.g.: protons 6 and 6') and for methine groups (e.g.: proton 5). Signals observed for strongly coupled protons, in contrast, show significant magnetization losses, leading to differentially broadened unsymmetrical heteronuclear doublets. Users should take this as an indication that the signal separation measured may not represent the heteronuclear coupling in this case and should use reasonably big uncertainties for the corresponding couplings or alternatively refrain from coupling constant extraction in these cases. Strong coupling can even lead to almost complete signal disappearance, as in the case of proton 3', with very poor definition of the actual peak positions. The appearance of different shapes of the heteronuclear doublet is a common feature of strongly coupled protons for the methods compared here.

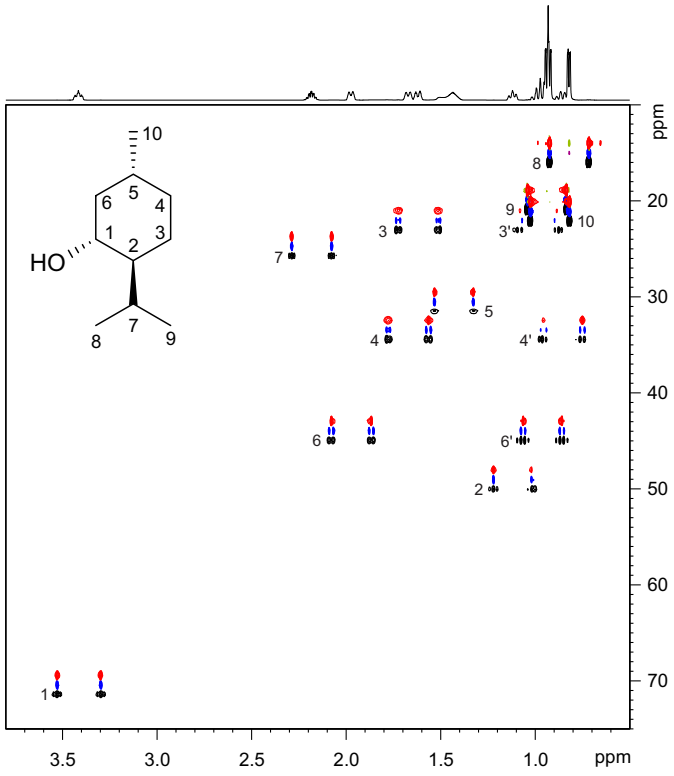

Figure S10: F_2 heterocoupled CLIP HSQC spectra of (1R, 2S, 5R)-(-)-menthol, 0.5 M in chloroform. The spectra were acquired without decoupling (black), with BIRD decoupling (blue) and with perfectBIRD decoupling (red) in the proton dimension. The BIRD and the perfectBIRD decoupled spectra were shifted along the carbon dimension for a clearer representation and a proton spectrum is shown atop the 2D spectra. The structure of the analyte is shown with the numbering used. For acquisition a11.4 T Bruker Avance III spectrometer equipped with a 5 mm TBI probe was used, operated by TopSpin 3.2 patchlevel 5. The sample temperature was regulated to 300K. All spectra were acquired with a spectral width of

4000 Hz (6.66 ppm) in the proton and with 10600 Hz (70.2 ppm) in the carbon dimension. The carrier frequencies were set to 2 ppm in the proton and to 45 ppm in the carbon dimension. In the experiment without homonuclear decoupling, 2048 complex data points were collected in the direct dimension throughout an acquisition of 0.512 s. For the homodecoupled experiments, 32 data chunks of each 10 ms length were collected and contracted to yield an FID of 0.32 s length (1280 complex points). The measurements were preceded by 32 dummy scans, while a two-step phase cycle was used throughout the measurements. INEPT and BIRD delays were optimized for one-bond coupling constants of 145 Hz and a recycle delay of 1 s was used. For proton and carbon hard excitation pulses of 9.5 µs and 13 µs were used respectively. All gradients used were smoothed square pulses (SMSQ10.100) of 1 ms duration, followed by a 200 µs gradient recovery delay. The gradients strengths used were G_1 = 15 %, G_2 = 80 %, G_3 = 11 %, G_4 = 20.1 %, G_5 = 8 %, G_6 = 17 % and G_7 = 90 % of the maximum gradient strength. The sign of G_2 was changed in alternate experiments according to the Echo-Antiecho procedure, to achieve F_1 sign discrimination in the ^{13}C dimension. CLIP/CLAP HSQC experiments without homonuclear decoupling, as proposed by Luy ***et al.***[2], only use G_2 and G_4. The experimental duration was 7 min 21 s for the experiment without decoupling, while the BIRD and perfectBIRD decoupled experiments required 3 h and 3 h 20 min, respectively.

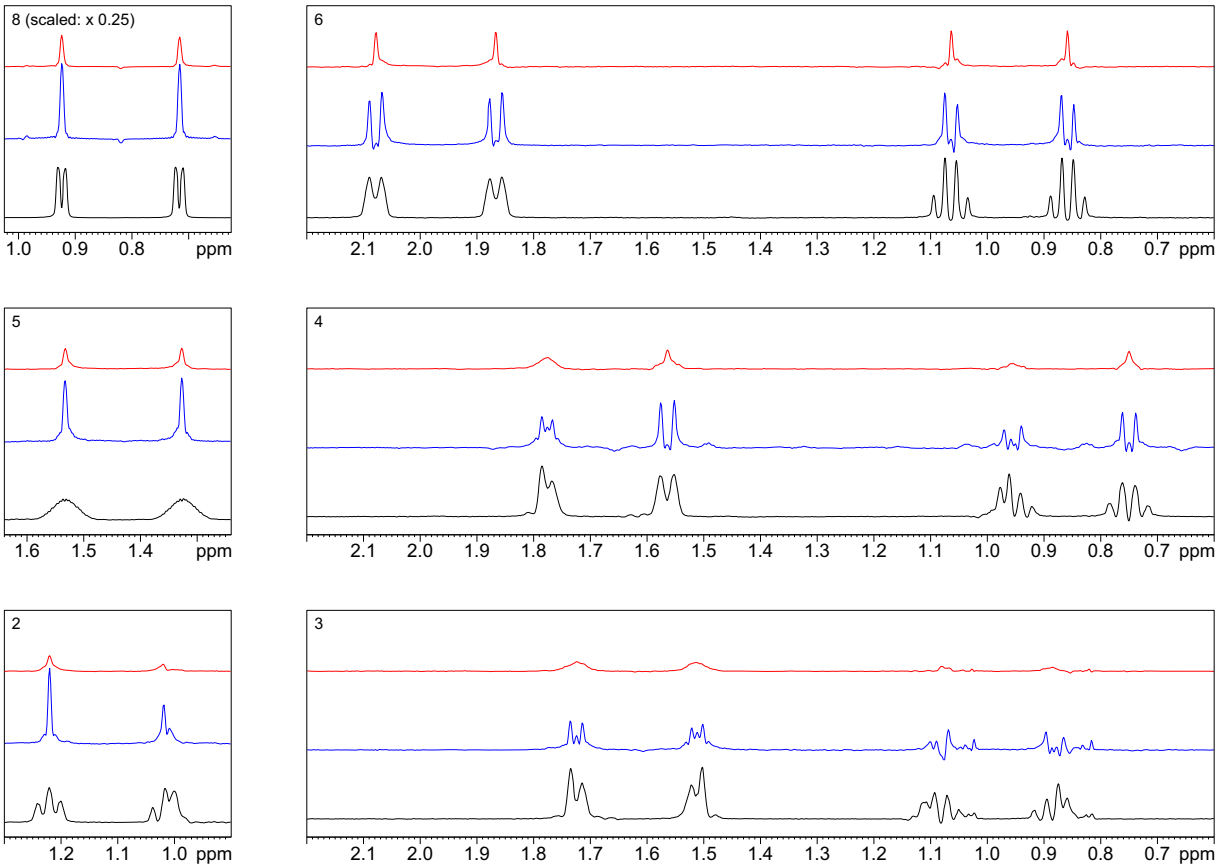

Figure S11: Traces extracted from the spectra shown in Figure S10 at different ^{13}C frequencies. Examples for weakly coupled protons can be found at the respective frequencies of C5 (methine group), C6 (methylene group) and C8 (methyl group). The effects of strong coupling are illustrated for the proton located at C2 (methine) as well as for the two methylene groups C3 and C4, covering various ranges of the strong coupling regime. All traces are shown at the same signal-to-noise ratio, as determined from an empty spectral region, except for the methyl signals (C8) which have been plotted with reduced intensity.

Pulse sequences for the F_2 heteronuclear coupled experiments presented

F_2 heteronuclear coupled F_2 perfectBIRD homodecoupled CLIP HSQC experiment

```
;hsqcCLIP_EA_pBIRD_F2cd.r1.7.lk                 ;lk 20140910
;based on hsqcCLIP_EA_pBIRD_F2cd.r1.6.lk                 ;lk 20140528
;DRX/AVANCE version
;HSQC
;2D H-1/X correlation via double inept transfer
;phase sensitive using echo/antiecho method
;with homonuclear decoupling during acquisition using perfect echo inserted BIRD decoupling (echo for 12C-bound protons too
in prefocusing period)
;the perfectBIRD prefocusing period can be set to a constant duration (t2'=0) (see ZGOPTNS at the end)
;using shaped pulses for inversion during the BIRD-elements
;using shaped pulses for inversion and refocussing on f2 - channel (not in BIRD-element)
;gradient filtration over perfect echo mixing pulse
;
;This pulse sequence is part of
;Lukas Kaltschnee, Andreas Kolmer, István Timári, Volker Schmidts, Ralph W. Adams,
;Mathias Nilsson, Katalin E. Kövér, Gareth A. Morris, and Christina M. Thiele,
;""Perfecting" pure shift HSQC: full homodecoupling for accurate and precise determination of heteronuclear couplings",
;manuscript in preparation
;
;The pulse sequence has been coded for test purposes only and
;may contain errors. It does contain arguments that can lead to
;hardware damages if acquisition parameters are set unfavorably.
;The functionality of the pulse sequence itself may differ depending on
;the hardware as well as the software used to execute it. Functionality
;on differing systems cannot be granted.
;Any use of this pulse sequence on a spectrometer is at your own risk.
;
;By using this pulse sequence, or any modification of it in any published material
;you agree to acknowledge the above-mentioned publication.
;
;Further publications relevant to this content:
;A. Enthart, J. C. Freudenberger, J. Furrer, H. Kessler, B. Luy, Journal of Magnetic Resonance 2008, 192, 314-322.
;P. Sakhaii, B. Haase, W. Bermel, Journal of Magnetic Resonance 2009, 199, 192-198.
;J. A. Aguilar, M. Nilsson, G. A. Morris, Angewandte Chemie International Edition 2011, 50, 9716-9717.
;I. Timári, L. Kaltschnee, A. Kolmer, R. W. Adams, M. Nilsson, C. M. Thiele, G. A. Morris, K. E. Kövér, Journal of Magnetic
Resonance 2014, 239, 130-138.
;T. Reinsperger, B. Luy, Journal of Magnetic Resonance 2014, 239, 110-120.
;

;$CLASS=HighRes
;$DIM=3D
;$TYPE=
;$SUBTYPE=
;$COMMENT=


#include <Avance.incl>
#include <Grad.incl>
#include <Delay.incl>

define delay tauA
define delay tauB
define delay tauC
define delay tauD
define delay tauE
define delay tauF
define delay tauG
define delay DBIRD

"p2=p1*2"
"p4=p3*2"

"d4=1s/(cnst2*4)"
"d3=1s/(cnst2*2)"

"DBIRD=d3-larger(p2, p14)/2"

"d11=30m"

#   ifdef LABEL_CN
"p22=p21*2"
#   else
#   endif /*LABEL_CN*/


#ifndef LABEL_DRX
          "in0=inf2/2"
          "d0=3u"
#else
          "d10=3u"
#endif

"DELTA1=d4-p16-larger(p2,p14)/2-8u-p3"
"DELTA2=d4-larger(p2,p14)/2"
#ifdef PI
          "DELTA3=d4-larger(p2,p14)/2-p1*2/PI"
#else
          "DELTA3=d4-larger(p2,p14)/2-p1*2/3.14159"
#endif


#ifdef LABEL_CN
#ifndef LABEL_DRX
          "DELTA=p16+d16+larger(p2,p22)+d0*2"
#else
```

```
          "DELTA=p16+d16+larger(p2,p22)+d10*2"
#endif /*LABEL_DRX*/
#   else  /*LABEL_CN*/
#ifndef LABEL_DRX
          "DELTA=p16+d16+p2+d0*2"
#else
          "DELTA=p16+d16+p2+d10*2"
#endif /*LABEL_DRX*/
#endif /*LABEL_CN*/

"cnst4=0"

#ifndef LABEL_DRX
          "in10=inf1/2"
          "d10=0"
#else
          "d0=0"
#endif
#ifndef LABEL_DRX
          "tauA=in10/2-p16*2-d16*2-50u"
          "tauB=in10/2+50u"
#else
          "tauA=in0/2-p16*2-d16*2-50u"
          "tauB=in0/2+50u"
#endif

#ifndef LABEL_DRX
          "tauD=in10*0.5-DELTA1/2-DELTA3/2-p14/2-p3/2-p1*0.75+d16*0.5+171u+larger(p1,p4)*0.25"
          "tauG=in10*0.5-p1*0.75+p16*0.5+d16*0.5+175u+larger(p1,p4)*0.25"
#else
          "tauD=in0*0.5-DELTA1/2-DELTA3/2-p14/2-p3/2-p1*0.75+d16*0.5+171u+larger(p1,p4)*0.25"
          "tauG=in0*0.5-p1*0.75+p16*0.5+d16*0.5+175u+larger(p1,p4)*0.25"
#endif

          "tauE=tauD-p16-d16"
          "tauF=tauG-p16-d16-50u"

aqseq 312

#ifndef LABEL_DRX
          "acqt0=0"
          baseopt_echo
#endif



1 ze
  d11

2 d1 do:f2
3 (p1 ph1)
  DELTA2 pl0:f2
  4u
  (center (p2 ph1) (p14:sp3 ph6):f2 )
  4u
  DELTA2 pl2:f2 UNBLKGRAD

  (p1 ph2)
  3u
  p16:gp3                     ;gpz3=15 purging gradient
  d16

  (p3 ph3):f2

#ifndef LABEL_DRX
          d0
#else
          d10
#endif

#ifdef LABEL_CN
  (center (p2 ph5) (p22 ph1):f3 )
#else
  (p2 ph5)
#endif /*LABEL_CN*/

#ifndef LABEL_DRX
          d0
#else
          d10
#endif

  p16:gp1*EA*-1
  d16 pl0:f2
  4u
  (p24:sp7 ph8):f2
  4u
  DELTA pl2:f2

  (p3 ph4):f2
  3u
  p16:gp4
  d16

  (p1 ph1)

  DELTA3 pl0:f2
  (center (p2 ph1) (p14:sp3 ph9):f2 )
  4u
  p16:gp2
  DELTA1 pl2:f2
  4u
  (p3 ph7):f2

#ifndef LABEL_CDUR
```

```
#ifndef LABEL_DRX
          d10*0.5
#else
          d0*0.5
#endif
#endif

  tauD
  p2 ph14

#ifndef LABEL_CDUR
#ifndef LABEL_DRX
          d10*0.5
#else
          d0*0.5
#endif
#endif

  tauE
  p16:gp19
  d16

  (p1 ph14)
  DBIRD pl0:f2
  (center (p2 ph14) (p14:sp3 ph10):f2)
  DBIRD pl2:f2
  (p1 ph14)

  50u
  p16:gp19
  d16
  tauF

#ifndef LABEL_CDUR
#ifndef LABEL_DRX
          d10*0.5
#else
          d0*0.5
#endif
#endif

  p2 ph14

  tauF

#ifndef LABEL_CDUR
#ifndef LABEL_DRX
          d10*0.5
#else
          d0*0.5
#endif
#endif

  50u
  p16:gp21*1
  d16

  (p1 ph15)

  50u
  p16:gp21*-1
  d16

#ifndef LABEL_DRX
          d10
#else
          d0
#endif

  tauA
  p16:gp20*0.25
  d16
  (p2 ph20)
  tauB
  p16:gp20*1.0
  d16
  300u

  (p1 ph11)
  DBIRD pl0:f2
  (center (p2 ph11) (p14:sp3 ph16):f2)
  DBIRD pl2:f2
  (p1 ph11) (p4 ph11):f2

  100u
  200u
  p16:gp20*0.75
  d16
  50u BLKGRAD

#ifndef LABEL_DRX
          d10
#else
          d0
#endif

4 go=2 ph31
  30u
  d1 do:f2 mc #0 to 2

#ifndef LABEL_DRX
  F1QF(caldel(d10, +in10))
  F2EA(calgrad(EA), caldel(d0, +in0) & calph(ph3, +180) & calph(ph6, +180) & calph(ph31, +180))
#else
  F1QF(id0)
```

```
  F2EA(rd0 & igrad EA, id10 & ip3*2 & ip6*2 & ip31*2)
#endif

exit

ph1=0
ph2=1
ph3=0 2
ph4=0 0 0 0 2 2 2 2
ph5=0
ph6=0
ph7=0 2
ph8=0 0 0 0 2 2 2 2
ph9=0
ph10=0
ph11= 1
ph12= 1
ph13= 2
ph14= 0
ph15= 1 1 3 3 1 1 3 3
ph16=1
ph20= 1
ph31= 0 2 0 2 2 0 2 0

;pl0: 0W
;pl1: f1 channel - power level for pulse (default)
;pl2: f2 channel - power level for pulse (default)
;pl3: f3 channel - power level for pulse (default)
;sp3: f2 channel - shaped pulse 180 degree for inversion
;spnam3: Crp60,0.5,20.1
;sp7: f2 channel - shaped pulse 180 degree for refocussing
;spnam7: Crp60comp.4
;p1: f1 channel -  90 degree high power pulse
;p2: f1 channel - 180 degree high power pulse
;p3: f2 channel -  90 degree high power pulse
;p14: f2 channel - 180 degree shaped pulse for inversion = 500usec for Crp60,0.5,20.1
;p16: homospoil/gradient pulse (1m)
;p21: f3 channel -  90 degree high power pulse
;p22: f3 channel - 180 degree high power pulse
;p24: f2 channel - 180 degree shaped pulse for refocussing = 2msec for Crp60comp.4
#ifndef LABEL_DRX
;d0: incremented delay (indirect dimension) [3 usec]
;d10: incremented delay (broadband decoupling dimension) [0 usec]
;inf2: 1/SW(F2) = 2 * DW(F2)
;inf1: n*DW(F3) << 2/J(HH)
;in0: 1/(2 * SW(F2)) = DW(F2)
;in10: inf1/2
#else
;d0: incremented delay (broadband decoupling dimension) [0 usec]
;d10: incremented delay (indirect dimension) [3 usec]
;in0: n*DW(F3) << 1/J(HH)
;in10: 1/(2 * SW(F2)) = DW(F2)
;nd0: 2
;nd10: 2
#endif
;d1: relaxation delay; 1-5 * T1
;d4: 1/(4J)XH
;d11: delay for disk I/O                             [30 msec]
;d16: delay for homospoil/gradient recovery
;cnst2: = J(XH)
;NS: 2 * n
;DS: >= 16
;td1: number of experiments
;1 FnMODE: QF
;2 FnMODE: Echo/Antiecho
;cnst4: 0

;use gradient ratio:          gp 1 : gp 2
;                               80 : 20.1    for C-13
;                               80 :  8.1    for N-15

;for z-only gradients:
;gpz1: 80%
;gpz2: 20.1% for C-13, 8.1% for N-15
;gpz3: 15%
;gpz4: 11%
;gpz19: 17%
;gpz20: 100% (spectrometer dependent)
;gpz21: 8%


;use gradient files:
;gpnam1: SMSQ10.100
;gpnam2: SMSQ10.100
;gpnam3: SMSQ10.100
;gpnam4: SMSQ10.100
;gpnam19: SMSQ10.100
;gpnam20: SMSQ10.100
;gpnam21: SMSQ10.100


                                        ;preprocessor-flags-start
;LABEL_CN: for C-13 and N-15 labeled samples start experiment with
;             option -DLABEL_CN (eda: ZGOPTNS)
;LABEL_DRX: when using this pulse sequence on DRX-machines start
;                            experiment with option -DLABEL_DRX (eda: ZGOPTNS)
;LABEL_CDUR: to use a constant duration for perfectBIRD prefocusing
;                            (t2'=0 instead of t2'=t2) start experiment with
;                            option -DLABEL_CDUR (eda: ZGOPTNS)
                                        ;preprocessor-flags-end
```

F_2 heteronuclear coupled F_2 perfectBIRD homodecoupled CLAP HSQC experiment

```
;hsqcCLAP_EA_pBIRD_F2cd.r1.7.lk                  ,lk 20140910
;based on hsqcCLAP_EA_pBIRD_F2cd.r1.6.lk                  ,lk 20140528
;DRX/AVANCE version
;HSQC
;2D H-1/X correlation via double inept transfer
;phase sensitive using echo/antiecho method
;with homonuclear decoupling during acquisition using perfect echo inserted BIRD decoupling (echo for 12C-bound protons too
in prefocusing period)
;using shaped pulses for inversion during the BIRD-elements
;using shaped pulses for inversion and refocussing on f2 - channel (not in BIRD-element)
;gradient filtration over perfect echo mixing pulse
;
;This pulse sequence is part of
;Lukas Kaltschnee, Andreas Kolmer, István Timári, Volker Schmidts, Ralph W. Adams,
;Mathias Nilsson, Katalin E. Kövér, Gareth A. Morris, and Christina M. Thiele,
;"“Perfecting” pure shift HSQC: full homodecoupling for accurate and precise determination of heteronuclear couplings",
;manuscript in preparation
;
;The pulse sequence has been coded for test purposes only and
;may contain errors. It does contain arguments that can lead to
;hardware damages if acquisition parameters are set unfavorably.
;The functionality of the pulse sequence itself may differ depending on
;the hardware as well as the software used to execute it. Functionality
;on differing systems cannot be granted.
;Any use of this pulse sequence on a spectrometer is at your own risk.
;
;By using this pulse sequence, or any modification of it in any published material
;you agree to acknowledge the above-mentioned publication.
;
;Further publications relevant to this content:
;A. Enthart, J. C. Freudenberger, J. Furrer, H. Kessler, B. Luy, Journal of Magnetic Resonance 2008, 192, 314-322.
;P. Sakhaii, B. Haase, W. Bermel, Journal of Magnetic Resonance 2009, 199, 192-198.
;J. A. Aguilar, M. Nilsson, G. A. Morris, Angewandte Chemie International Edition 2011, 50, 9716-9717.
;I. Timári, L. Kaltschnee, A. Kolmer, R. W. Adams, M. Nilsson, C. M. Thiele, G. A. Morris, K. E. Kövér, Journal of Magnetic
Resonance 2014, 239, 130-138.
;T. Reinsperger, B. Luy, Journal of Magnetic Resonance 2014, 239, 110-120.
;

;$CLASS=HighRes
;$DIM=3D
;$TYPE=
;$SUBTYPE=
;$COMMENT=


#include <Avance.incl>
#include <Grad.incl>
#include <Delay.incl>

define delay tauA
define delay tauB
define delay tauC
define delay tauD
define delay tauE
define delay tauF
define delay tauG
define delay DBIRD

"p2=p1*2"
"p4=p3*2"

"d4=1s/(cnst2*4)"
"d3=1s/(cnst2*2)"

"DBIRD=d3-larger(p2, p14)/2"

"d11=30m"

"d7=p16+d16+4u"

#   ifdef LABEL_CN
"p22=p21*2"
#   else
#   endif /*LABEL_CN*/

#ifndef LABEL_DRX
         "in0=inf2/2"
         "d0=3u"
#else
         "d10=3u"
#endif

"DELTA1=d4-p16-larger(p2,p14)/2-de-8u"
"DELTA2=d4-larger(p2,p14)/2"
#ifdef PI
         "DELTA3=d4-larger(p2,p14)/2-p1*2/PI"
#else
         "DELTA3=d4-larger(p2,p14)/2-p1*2/3.14159"
#endif

#ifdef LABEL_CN
#ifndef LABEL_DRX
         "DELTA=p16+d16+larger(p2,p22)+d0*2"
#else
         "DELTA=p16+d16+larger(p2,p22)+d10*2"
#endif /*LABEL_DRX*/
#   else  /*LABEL_CN*/
#ifndef LABEL_DRX
         "DELTA=p16+d16+p2+d0*2"
#else
         "DELTA=p16+d16+p2+d10*2"
#endif /*LABEL_DRX*/
```

```
#endif /*LABEL_CN*/

"cnst4=0"

#ifndef LABEL_DRX
          "in10=inf1/2"
          "d10=0"
#else
          "d0=0"
#endif
#ifndef LABEL_DRX
          "tauA=in10/2-p16*2-d16*2-50u"
          "tauB=in10/2+50u"
#else
          "tauA=in0/2-p16*2-d16*2-50u"
          "tauB=in0/2+50u"
#endif

#ifndef LABEL_DRX
          "tauD=in10*0.5-d7-p1*1.75+p16*0.5+d16*0.5+175u+larger(p1,p4)*0.25"
          "tauG=in10*0.5-p1*0.75+p16*0.5+d16*0.5+175u+larger(p1,p4)*0.25"
#else
          "tauD=in0*0.5-d7-p1*1.75+p16*0.5+d16*0.5+175u+larger(p1,p4)*0.25"
          "tauG=in0*0.5-p1*0.75+p16*0.5+d16*0.5+175u+larger(p1,p4)*0.25"
#endif

          "tauE=tauD-p16-d16"
          "tauF=tauG-p16-d16-50u"

aqseq 312

#ifndef LABEL_DRX
          "acqt0=0"
          baseopt_echo
#endif



1 ze
  d11

2 d1 do:f2
3 (p1 ph1)
  DELTA2 pl0:f2
  4u
  (center (p2 ph1) (p14:sp3 ph6):f2 )
  4u
  DELTA2 pl2:f2 UNBLKGRAD

  (p1 ph2)
  3u
  p16:gp3
  d16

  (p3 ph3):f2

#ifndef LABEL_DRX
          d0
#else
          d10
#endif

#ifdef LABEL_CN
  (center (p2 ph5) (p22 ph1):f3 )
#else
  (p2 ph5)
#endif /*LABEL_CN*/

#ifndef LABEL_DRX
          d0
#else
          d10
#endif

  p16:gp1*EA*-1
  d16 pl0:f2
  4u
  (p24:sp7 ph8):f2
  4u
  DELTA pl2:f2

  (p3 ph4):f2
  3u
  p16:gp4
  d16
  (p1 ph1)

  d7

  p2 ph1
  4u
  p16:gp2                    ;gpz2 for coherence selection: gpz1 = 80, gpz2 = 20.1 for 13C/1H
  d16

#ifndef LABEL_DRX
          d10*0.5
#else
          d0*0.5
#endif

  tauD

  p2 ph14

#ifndef LABEL_DRX
```

```
          d10*0.5
#else
          d0*0.5
#endif

  tauE
  p16:gp19
  d16

  (p1 ph14)
  DBIRD pl0:f2
  (center (p2 ph14) (p14:sp3 ph10):f2)
  DBIRD pl2:f2
  (p1 ph14)

  50u
  p16:gp19
  d16
  tauF

#ifndef LABEL_DRX
          d10*0.5
#else
          d0*0.5
#endif

  p2 ph14

  tauF

#ifndef LABEL_DRX
          d10*0.5
#else
          d0*0.5
#endif

  50u
  p16:gp21*1
  d16

  (p1 ph15)

  50u
  p16:gp21*-1
  d16

#ifndef LABEL_DRX
          d10
#else
          d0
#endif

  tauA
  p16:gp20*0.25
  d16
  (p2 ph20)
  tauB
  p16:gp20*1.0
  d16
  300u

  (p1 ph11)
  DBIRD pl0:f2
  (center (p2 ph11) (p14:sp3 ph16):f2)
  DBIRD pl2:f2
  (p1 ph11) (p4 ph11):f2

  100u
  200u
  p16:gp20*0.75
  d16
  50u BLKGRAD

#ifndef LABEL_DRX
          d10
#else
          d0
#endif

4 go=2 ph31
  30u
  d1 do:f2 mc #0 to 2

#ifndef LABEL_DRX
  F1QF(caldel(d10, +in10))
  F2EA(calgrad(EA), caldel(d0, +in0) & calph(ph3, +180) & calph(ph6, +180) & calph(ph31, +180))

#else
  F1QF(id0)
  F2EA(rd0 & igrad EA, id10 & ip3*2 & ip6*2 & ip31*2)

#endif

exit

ph1=0
ph2=1
ph3=0 2
ph4=0 0 0 0 2 2 2 2
ph5=0
ph6=0
ph7=0 2
ph8=0 0 0 0 2 2 2 2
ph10=0
ph11= 1
```

```
ph12= 1
ph13= 2
ph14= 0
ph15= 1 1 3 3 1 1 3 3
ph16=1
ph20= 1
ph31= 0 2 0 2 2 0 2 0

;pl0: 0W
;pl1: f1 channel - power level for pulse (default)
;pl2: f2 channel - power level for pulse (default)
;pl3: f3 channel - power level for pulse (default)
;sp3: f2 channel - shaped pulse 180 degree for inversion
;spnam3: Crp60,0.5,20.1
;sp7: f2 channel - shaped pulse 180 degree for refocussing
;spnam7: Crp60comp.4
;p1: f1 channel -  90 degree high power pulse
;p2: f1 channel - 180 degree high power pulse
;p3: f2 channel -  90 degree high power pulse
;p14: f2 channel - 180 degree shaped pulse for inversion = 500usec for Crp60,0.5,20.1
;p16: homospoil/gradient pulse (1m)
;p21: f3 channel -  90 degree high power pulse
;p22: f3 channel - 180 degree high power pulse
;p24: f2 channel - 180 degree shaped pulse for refocussing = 2msec for Crp60comp.4
#ifndef LABEL_DRX
;d0: incremented delay (indirect dimension) [3 usec]
;d10: incremented delay (broadband decoupling dimension) [0 usec]
;inf2: 1/SW(F2) = 2 * DW(F2)
;inf1: n*DW(F3) << 2/J(HH)
;in0: 1/(2 * SW(F2)) = DW(F2)
;in10: inf1/2
#else
;d0: incremented delay (broadband decoupling dimension) [0 usec]
;d10: incremented delay (indirect dimension) [3 usec]
;in0: n*DW(F3) << 1/J(HH)
;in10: 1/(2 * SW(F2)) = DW(F2)
;nd0: 2
;nd10: 2
#endif
;d1: relaxation delay; 1-5 * T1
;d4: 1/(4J)XH
;d7: p16+d16+4u
;d11: delay for disk I/O                             [30 msec]
;d16: delay for homospoil/gradient recovery
;cnst2: = J(XH)
;NS: 2 * n
;DS: >= 16
;td1: number of experiments
;1 FnMODE: QF
;2 FnMODE: echo/antiecho
;cnst4: 0

;use gradient ratio:          gp 1 : gp 2
;                               80 : 20.1    for C-13
;                               80 :  8.1    for N-15

;for z-only gradients:
;gpz1: 80%
;gpz2: 20.1% for C-13, 8.1% for N-15
;gpz3: 15%
;gpz4: 11%
;gpz19: 17%
;gpz20: 100% (spectrometer dependent)
;gpz20: 8%

;use gradient files:
;gpnam1: SMSQ10.100
;gpnam2: SMSQ10.100
;gpnam3: SMSQ10.100
;gpnam4: SMSQ10.100
;gpnam19: SMSQ10.100
;gpnam20: SMSQ10.100
;gpnam21: SMSQ10.100

                                        ;preprocessor-flags-start
;LABEL_CN: for C-13 and N-15 labeled samples start experiment with
;             option -DLABEL_CN (eda: ZGOPTNS)
;LABEL_DRX: when using this pulse sequence on DRX-machines start
;                              experiment with option -DLABEL_DRX (eda: ZGOPTNS)
                                        ;preprocessor-flags-end
```

F_2 heteronuclear coupled F_2 BIRD homodecoupled CLIP HSQC experiment

```
;hsqcCLIP_EA_BIRD_F2cd.r1.7.lk                  ;lk 20140910
;based on hsqcCLIP_EA_BIRD_F2cd.r1.6.lk                  ;lk 20140528
;DRX/AVANCE version
;HSQC
;2D H-1/X correlation via double inept transfer
;phase sensitive using echo/antiecho method
;with homonuclear BIRD decoupling during acquisition
;using shaped pulses for inversion during the BIRD-element
;using shaped pulses for inversion and refocussing on f2 - channel (not in BIRD-element)
;
;This pulse sequence is part of
;Lukas Kaltschnee, Andreas Kolmer, István Timári, Volker Schmidts, Ralph W. Adams,
;Mathias Nilsson, Katalin E. Kövér, Gareth A. Morris, and Christina M. Thiele,
;""Perfecting" pure shift HSQC: full homodecoupling for accurate and precise determination of heteronuclear couplings",
;manuscript in preparation
;
;The pulse sequence has been coded for test purposes only and
;may contain errors. It does contain arguments that can lead to
```

```
;hardware damages if acquisition parameters are set unfavorably.
;The functionality of the pulse sequence itself may differ depending on
;the hardware as well as the software used to execute it. Functionality
;on differing systems cannot be granted.
;Any use of this pulse sequence on a spectrometer is at your own risk.
;
;By using this pulse sequence, or any modification of it in any published material
;you agree to acknowledge the above-mentioned publication.
;
;Further publications relevant to this content:
;A. Enthart, J. C. Freudenberger, J. Furrer, H. Kessler, B. Luy, Journal of Magnetic Resonance 2008, 192, 314-322.
;P. Sakhaii, B. Haase, W. Bermel, Journal of Magnetic Resonance 2009, 199, 192-198.
;J. A. Aguilar, M. Nilsson, G. A. Morris, Angewandte Chemie International Edition 2011, 50, 9716-9717.
;I. Timári, L. Kaltschnee, A. Kolmer, R. W. Adams, M. Nilsson, C. M. Thiele, G. A. Morris, K. E. Kövér, Journal of Magnetic
Resonance 2014, 239, 130-138.
;T. Reinsperger, B. Luy, Journal of Magnetic Resonance 2014, 239, 110-120.
;

;$CLASS=HighRes
;$DIM=3D
;$TYPE=
;$SUBTYPE=
;$COMMENT=

#include <Avance.incl>
#include <Grad.incl>
#include <Delay.incl>

define delay tauA
define delay tauB
define delay tauC
define delay DBIRD

"p2=p1*2"
"p4=p3*2"

"d4=1s/(cnst2*4)"
"d3=1s/(cnst2*2)"

"DBIRD=d3-larger(p2, p14)/2"

"d11=30m"

#   ifdef LABEL_CN
"p22=p21*2"
#   else
#   endif /*LABEL_CN*/

#ifndef LABEL_DRX
          "in0=inf2/2"
          "d0=3u"
#else
          "d10=3u"
#endif

"DELTA1=d4-p16-larger(p2,p14)/2-de-8u"
"DELTA2=d4-larger(p2,p14)/2"
#ifdef PI
          "DELTA3=d4-larger(p2,p14)/2-p1*2/PI"
#else
          "DELTA3=d4-larger(p2,p14)/2-p1*2/3.14159"
#endif

#   ifdef LABEL_CN
#ifndef LABEL_DRX
          "DELTA=p16+d16+larger(p2,p22)+d0*2"
#else
          "DELTA=p16+d16+larger(p2,p22)+d10*2"
#endif /*LABEL_DRX*/
#   else
#ifndef LABEL_DRX
          "DELTA=p16+d16+p2+d0*2"
#else
          "DELTA=p16+d16+p2+d0*2"
#endif /*LABEL_DRX*/
#endif /*LABEL_CN*/

"cnst4=0"

#ifndef LABEL_DRX
          "in10=inf1/2"
          "d10=0"
#else
          "d0=0"
#endif
#ifndef LABEL_DRX
          "tauA=in10/2-p16-d16-50u"
          "tauB=in10/2+50u"
#else
          "tauA=in0/2-p16-d16-50u"
          "tauB=in0/2+50u"
#endif

aqseq 312

#ifndef LABEL_DRX
          "acqt0=0"
          baseopt_echo
#endif


1 ze
  d11

2 d1 do:f2
```

```
3 (p1 ph1)
  DELTA2 pl0:f2
  4u
  (center (p2 ph1) (p14:sp3 ph6):f2 )
  4u
  DELTA2 pl2:f2 UNBLKGRAD

  (p1 ph2)
  3u
  p16:gp3
  d16

  (p3 ph3):f2

#ifndef LABEL_DRX
          d0
#else
          d10
#endif

#ifdef LABEL_CN
  (center (p2 ph5) (p22 ph1):f3 )
#else
  (p2 ph5)
#endif /*LABEL_CN*/

#ifndef LABEL_DRX
          d0
#else
          d10
#endif

  p16:gp1*EA
  d16 pl0:f2
  4u
  (p24:sp7 ph8):f2
  4u
  DELTA pl2:f2

  (p3 ph4):f2
  3u
  p16:gp4
  d16

  (p1 ph1)

  DELTA3 pl0:f2
  (center (p2 ph1) (p14:sp3 ph9):f2 )
  4u
  p16:gp2     ;gpz2 for coherence selection: gpz1 = 80, gpz2 = 20.1 for 13C/1H
  DELTA1 pl2:f2
  4u
  (p3 ph7):f2

#ifndef LABEL_DRX
          d10
#else
          d0
#endif

  tauA
  50u
  p16:gp20*0.25
  d16
  (p2 ph20)
  tauB
  p16:gp20*1.0
  d16

  300u

  (p1 ph11)
  DBIRD pl0:f2
  (center (p2 ph11) (p14:sp3 ph16):f2)
  DBIRD pl2:f2
  (p1 ph11) (p4 ph11):f2

  100u
  200u
  p16:gp20*0.75
  d16
  50u BLKGRAD

#ifndef LABEL_DRX
          d10
#else
          d0
#endif

4 go=2 ph31
  30u
  d1 do:f2 mc #0 to 2

#ifndef LABEL_DRX
  F1QF(caldel(d10, +in10))
  F2EA(calgrad(EA), caldel(d0, +in0) & calph(ph3, +180) & calph(ph6, +180) & calph(ph31, +180))
#else
  F1QF(id0)
  F2EA(rd0 & igrad EA, id10 & ip3*2 & ip6*2 & ip31*2)
#endif

exit

ph1=0
ph2=1
```

```
ph3=0 2
ph4=0 0 2 2
ph5=0
ph6=0
ph7=0 2
ph8=0 0 2 2
ph9=0
ph11= 1 1 1 1 2 2 2 2
ph12= 1
ph13= 2
ph16= 1 1 1 1 2 2 2 2
ph20=1 1 1 1 1 1 1 1 2 2 2 2 2 2 2 2
ph31=0 2 2 0 2 0 0 2 2 0 0 2 0 2 2 0

;pl0 : 0W
;pl1 : f1 channel - power level for pulse (default)
;pl2 : f2 channel - power level for pulse (default)
;pl3 : f3 channel - power level for pulse (default)
;sp3: f2 channel - shaped pulse 180 degree for inversion
;spnam3: Crp60,0.5,20.1
;sp7: f2 channel - shaped pulse 180 degree for refocussing
;spnam7: Crp60comp.4
;p1 : f1 channel -  90 degree high power pulse
;p2 : f1 channel - 180 degree high power pulse
;p3 : f2 channel -  90 degree high power pulse
;p14: f2 channel - 180 degree shaped pulse for inversion
;      = 500usec for Crp60,0.5,20.1
;p16: homospoil/gradient pulse (1m)
;p21 : f3 channel -  90 degree high power pulse
;p22: f3 channel - 180 degree high power pulse
;p24: f2 channel - 180 degree shaped pulse for refocussing
;      = 2msec for Crp60comp.4
#ifndef LABEL_DRX
;d0: incremented delay (indirect dimension) [3 usec]
;d10: incremented delay (broadband decoupling dimension) [0 usec]
;inf2: 1/SW(F2) = 2 * DW(F2)
;inf1: n*DW(F3) << 2/J(HH)
;in0: 1/(2 * SW(F2)) = DW(F2)
;in10: inf1/2
#else
;d0: incremented delay (broadband decoupling dimension) [0 usec]
;d10: incremented delay (indirect dimension) [3 usec]
;in0: n*DW(F3) << 1/J(HH)
;in10: 1/(2 * SW(F2)) = DW(F2)
;nd0: 2
;nd10: 2
#endif
;d1 : relaxation delay; 1-5 * T1
;d4 : 1/(4J)XH
;d11: delay for disk I/O                              [30 msec]
;d16: delay for homospoil/gradient recovery
;cnst2: = J(XH)
;NS: 2 * n
;DS: >= 16
;td1: number of experiments
;1 FnMODE: QF
;2 FnMODE: echo-antiecho
;cnst4: 0

;use gradient ratio:          gp 1 : gp 2
;                               80 : 20.1    for C-13
;                               80 :  8.1    for N-15

;for z-only gradients:
;gpz1: 80%
;gpz2: 20.1% for C-13, 8.1% for N-15
;gpz3: 15%
;gpz4: 11%
;gpz20: 100% (spectrometer dependent)


;use gradient files:
;gpnam1: SMSQ10.100
;gpnam2: SMSQ10.100
;gpnam3: SMSQ10.100
;gpnam4: SMSQ10.100
;gpnam20: SMSQ10.100


                                        ;preprocessor-flags-start
;LABEL_CN: for C-13 and N-15 labeled samples start experiment with
;          option -DLABEL_CN (eda: ZGOPTNS)
;LABEL_DRX: when using this pulse sequence on DRX-machines start
;                              experiment with option -DLABEL_DRX (eda: ZGOPTNS)
                                        ;preprocessor-flags-end
```

F_2 heteronuclear coupled F_2 BIRD homodecoupled CLAP HSQC experiment

```
;hsqcCLAP_EA_BIRD_F2cd.r1.7.lk                  ;lk 20140910
;based on hsqcCLAP_EA_BIRD_F2cd.r1.6.lk                  ;lk 20140528
;DRX/AVANCE version
;HSQC
;2D H-1/X correlation via double inept transfer
;phase sensitive using echo/antiecho method
;with homonuclear BIRD decoupling during acquisition
;using shaped pulses for inversion during the BIRD-element
;using shaped pulses for inversion and refocussing on f2 - channel (not in BIRD-element)
;
;This pulse sequence is part of
;Lukas Kaltschnee, Andreas Kolmer, István Timári, Volker Schmidts, Ralph W. Adams,
;Mathias Nilsson, Katalin E. Kövér, Gareth A. Morris, and Christina M. Thiele,
;"“Perfecting” pure shift HSQC: full homodecoupling for accurate and precise determination of heteronuclear couplings",
;manuscript in preparation
;
;The pulse sequence has been coded for test purposes only and
;may contain errors. It does contain arguments that can lead to
;hardware damages if acquisition parameters are set unfavorably.
;The functionality of the pulse sequence itself may differ depending on
;the hardware as well as the software used to execute it. Functionality
;on differing systems cannot be granted.
;Any use of this pulse sequence on a spectrometer is at your own risk.
;
;By using this pulse sequence, or any modification of it in any published material
;you agree to acknowledge the above-mentioned publication.
;
;Further publications relevant to this content:
;A. Enthart, J. C. Freudenberger, J. Furrer, H. Kessler, B. Luy, Journal of Magnetic Resonance 2008, 192, 314-322.
;P. Sakhaii, B. Haase, W. Bermel, Journal of Magnetic Resonance 2009, 199, 192-198.
;J. A. Aguilar, M. Nilsson, G. A. Morris, Angewandte Chemie International Edition 2011, 50, 9716-9717.
;I. Timári, L. Kaltschnee, A. Kolmer, R. W. Adams, M. Nilsson, C. M. Thiele, G. A. Morris, K. E. Kövér, Journal of Magnetic
Resonance 2014, 239, 130-138.
;T. Reinsperger, B. Luy, Journal of Magnetic Resonance 2014, 239, 110-120.
;

;$CLASS=HighRes
;$DIM=3D
;$TYPE=
;$SUBTYPE=
;$COMMENT=


#include <Avance.incl>
#include <Grad.incl>
#include <Delay.incl>

define delay tauA
define delay tauB
define delay tauC
define delay DBIRD

"p2=p1*2"
"p4=p3*2"

"d4=1s/(cnst2*4)"
"d3=1s/(cnst2*2)"

"DBIRD=d3-larger(p2, p14)/2"

"d11=30m"

"d7=p16+d16+4u"

#ifdef LABEL_CN
         "p22=p21*2"
#else
#endif /*LABEL_CN*/

#ifndef LABEL_DRX
         "in0=inf2/2"
         "d0=3u"
#else
         "d10=3u"
#endif

"DELTA1=d4-p16-larger(p2,p14)/2-de-8u"
"DELTA2=d4-larger(p2,p14)/2"
#ifdef PI
         "DELTA3=d4-larger(p2,p14)/2-p1*2/PI"
#else
         "DELTA3=d4-larger(p2,p14)/2-p1*2/3.14159"
#endif

#ifdef LABEL_CN
#ifndef LABEL_DRX
         "DELTA=p16+d16+larger(p2,p22)+d0*2"
#else
         "DELTA=p16+d16+larger(p2,p22)+d10*2"
#endif /*LABEL_DRX*/
#   else
#ifndef LABEL_DRX
         "DELTA=p16+d16+p2+d0*2"
#else
         "DELTA=p16+d16+p2+d0*2"
#endif /*LABEL_DRX*/
#endif /*LABEL_CN*/

"cnst4=0"

#ifndef LABEL_DRX
         "in10=inf1/2"
```

```
          "d10=0"
#else
          "d0=0"
#endif

#ifndef LABEL_DRX
          "tauA=in10/2-p16-d16-50u"
          "tauB=in10/2+50u"
#else
          "tauA=in0/2-p16-d16-50u"
          "tauB=in0/2+50u"
#endif

aqseq 312

#ifndef LABEL_DRX
          "acqt0=0"
          baseopt_echo
#endif


1 ze
  d11

2 d1 do:f2
3 (p1 ph1)
  DELTA2 pl0:f2
  4u
  (center (p2 ph1) (p14:sp3 ph6):f2 )
  4u
  DELTA2 pl2:f2 UNBLKGRAD

  (p1 ph2)
  3u
  p16:gp3
  d16

  (p3 ph3):f2

#ifndef LABEL_DRX
          d0
#else
          d10
#endif

#   ifdef LABEL_CN
  (center (p2 ph5) (p22 ph1):f3 )
#   else
  (p2 ph5)
#   endif /*LABEL_CN*/

#ifndef LABEL_DRX
          d0
#else
          d10
#endif

  p16:gp1*EA
  d16 pl0:f2
  4u
  (p24:sp7 ph8):f2
  4u
  DELTA pl2:f2

  (p3 ph4):f2
  3u
  p16:gp4
  d16

  (p1 ph1)

  d7
  p2 ph1
  4u
  p16:gp2                    ;gpz2 for coherence selection: gpz1 = 80, gpz2 = 20.1 for 13C/1H
  d16

#ifndef LABEL_DRX
          d10
#else
          d0
#endif

  tauA
  50u
  p16:gp20*0.25
  d16
  (p2 ph20)
  tauB
  p16:gp20*1.0
  d16
  300u

  (p1 ph11)
  DBIRD pl0:f2
  (center (p2 ph11) (p14:sp3 ph16):f2)
  DBIRD pl2:f2
  (p1 ph11) (p4 ph11):f2

  100u
  200u
  p16:gp20*0.75
  d16
  50u BLKGRAD
```

```
#ifndef LABEL_DRX
         d10
#else
         d0
#endif

4 go=2 ph31
  30u
  d1 do:f2 mc #0 to 2

#ifndef LABEL_DRX
  F1QF(caldel(d10, +in10))
  F2EA(calgrad(EA), caldel(d0, +in0) & calph(ph3, +180) & calph(ph6, +180) & calph(ph31, +180))
#else
  F1QF(id0)
  F2EA(rd0 & igrad EA, id10 & ip3*2 & ip6*2 & ip31*2)
#endif

exit

ph1=0
ph2=1
ph3=0 2
ph4=0 0 2 2
ph5=0
ph6=0
ph7=0 2
ph8=0 0 2 2
ph11= 1 1 1 1 2 2 2 2
ph12= 1
ph13= 2
ph16= 1 1 1 1 2 2 2 2
ph20=1 1 1 1 1 1 1 1 2 2 2 2 2 2 2 2
ph31=0 2 2 0 2 0 0 2 2 0 0 2 0 2 2 0

;pl0 : 0Ws
;pl1 : f1 channel - power level for pulse (default)
;pl2 : f2 channel - power level for pulse (default)
;pl3 : f3 channel - power level for pulse (default)
;sp3: f2 channel - shaped pulse 180 degree for inversion
;spnam3: Crp60,0.5,20.1
;sp7: f2 channel - shaped pulse 180 degree for refocussing
;spnam7: Crp60comp.4
;p1 : f1 channel -  90 degree high power pulse
;p2 : f1 channel - 180 degree high power pulse
;p3 : f2 channel -  90 degree high power pulse
;p14: f2 channel - 180 degree shaped pulse for inversion
;      = 500usec for Crp60,0.5,20.1
;p16: homospoil/gradient pulse (1m)
;p21 : f3 channel -  90 degree high power pulse
;p22: f3 channel - 180 degree high power pulse
;p24: f2 channel - 180 degree shaped pulse for refocussing
;      = 2msec for Crp60comp.4
#ifndef LABEL_DRX
;d0: incremented delay (indirect dimension) [3 usec]
;d10: incremented delay (broadband decoupling dimension) [0 usec]
;inf2: 1/SW(F2) = 2 * DW(F2)
;inf1: n*DW(F3) << 2/J(HH)
;in0: 1/(2 * SW(F2)) = DW(F2)
;in10: inf1/2
#else
;d0: incremented delay (broadband decoupling dimension) [0 usec]
;d10: incremented delay (indirect dimension) [3 usec]
;in0: n*DW(F3) << 1/J(HH)
;in10: 1/(2 * SW(F2)) = DW(F2)
;nd0: 2
;nd10: 2
#endif
;d1 : relaxation delay; 1-5 * T1
;d4 : 1/(4J)XH
;d11: delay for disk I/O                              [30 msec]
;d16: delay for homospoil/gradient recovery
;cnst2: = J(XH)
;NS: 2 * n
;DS: >= 16
;td1: number of experiments
;1 FnMODE: QF
;2 FnMODE: echo-antiecho
;cnst4: 0

;use gradient ratio:         gp 1 : gp 2
;                              80 : 20.1    for C-13
;                              80 :  8.1    for N-15

;for z-only gradients:
;gpz1: 80%
;gpz2: 20.1% for C-13, 8.1% for N-15
;gpz3: 15%
;gpz4: 11%
;gpz20: 100% (spectrometer dependent)

;use gradient files:
;gpnam1: SMSQ10.100
;gpnam2: SMSQ10.100
;gpnam3: SMSQ10.100
;gpnam4: SMSQ10.100
;gpnam20: SMSQ10.100

                                        ;preprocessor-flags-start
;LABEL_CN: for C-13 and N-15 labeled samples start experiment with
;             option -DLABEL_CN (eda: ZGOPTNS)
;LABEL_DRX: when using this pulse sequence on DRX-machines start
;                            experiment with option -DLABEL_DRX (eda: ZGOPTNS)
                                        ;preprocessor-flags-end
```

Spectra collected with $t'_2 = 0$ at 400 MHz proton frequency

As mentioned in the caption of Figure 1 of the main text, setting $t'_2 = 0$ for all values of t_2 can be used to recover the splittings from geminal couplings, while getting around the distortion of the methylene signals by coupling evolution prior to acquisition. Clear in-phase signals are expected in this case, if the geminal protons are weakly coupled. The perfect echo element is used in this case with a constant length to compensate for the inevitable delays during the BIRD decoupling element in which no net chemical shift evolution occurs. As can be seen from the figures shown below, the geminal splitting is retained for all four methylene protons in the test substance with significantly reduced distortion of the signal by coupling evolution (compare to the BIRD decoupled spectra in Figure S3 and Figure S6). The signals are however not obtained in fully absorptive lineshape, which may be attributable to strong coupling effects, particularly in the case of the aligned sample.

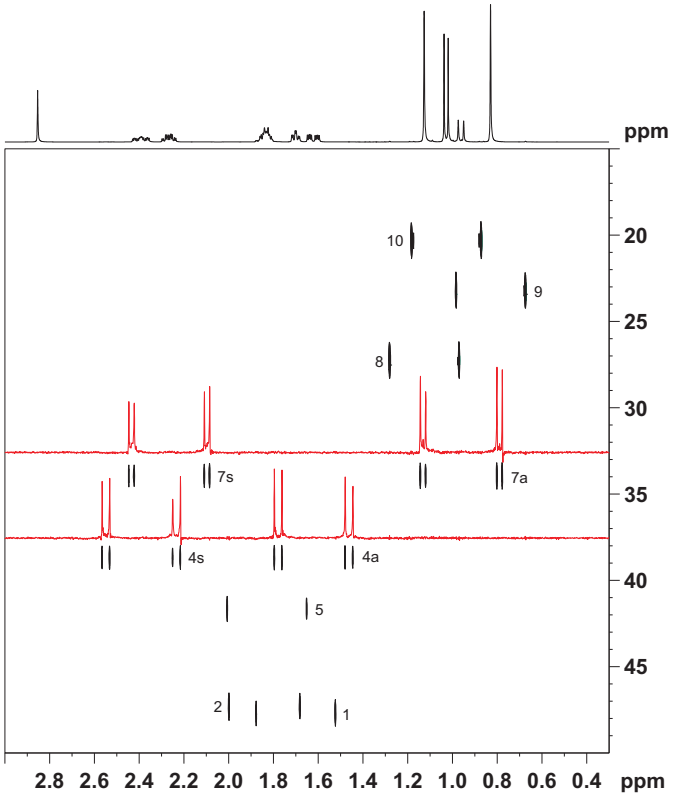

Figure S12: F_2 perfectBIRD decoupled CLIP HSQC spectrum of (+)-IPC dissolved in isotropic CD_2Cl_2 solution obtained by setting $t'_2 = 0$. Traces along the proton dimension are shown in red for the four methylene protons. Proton 3 is not shown for clearer representation. The spectrum was acquired with spectral widths of 10.4 ppm in the proton and 70 ppm in the carbon dimension. 48 data chunks of 19.2 ms length (160 • direct acquisition dwell time, *sw*2 = 52.1 Hz) were collected in the proton dimension for each increment in the indirect dimension, to construct an FID of 0.92 s length (3840 complex data points) in the proton dimension. 128 increments were collected in the carbon dimension. The measurement was preceded by 16 dummy scans, while a two-step phase cycle was used throughout the measurement. INEPT and BIRD delays were optimized for one-bond coupling constants of 125 Hz. A recycle delay of 1 s was used. The experimental duration was 5.4 h.

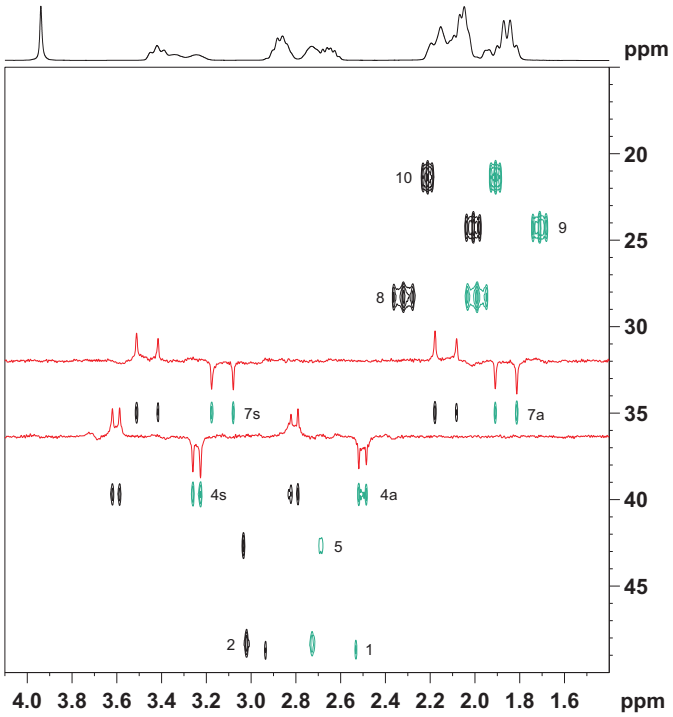

Figure S13: F_2 perfectBIRD decoupled CLAP HSQC spectrum of (+)-IPC dissolved in anisotropic CD_2Cl_2/PBDG solution obtained by setting $t'_2 = 0$. Traces along the proton dimension are shown in red for the four methylene protons. Proton 3 is not shown for clearer representation. The spectrum was acquired with spectral widths of 10.4 ppm in the proton and 70 ppm in the carbon dimension. 32 data chunks of 10.08 ms length (84 • direct acquisition dwell time, *sw*2 = 99.2 Hz) were collected in the proton dimension for each increment in the indirect dimension to construct an FID of 0.32 s length (1344 complex data points) in the direct dimension. 128 increments were collected in the carbon dimension. The measurement was preceded by 16 dummy scans, while a two-step phase cycle was used throughout the measurement. INEPT and BIRD delays were optimized for one-bond coupling constants of 125 Hz. A recycle delay of 1 s was used. The experimental duration was 2.9 h.

Literature

[1] A. Marx, C. Thiele, *Chem. Eur. J.* **2009**, *15*, 254-260.

[2] A. Enthart, J. C. Freudenberger, J. Furrer, H. Kessler, B. Luy, *J. Magn. Reson.* **2008**, *192*, 314-322.

[3] G. Kummerlöwe, S. Schmitt, B. Luy, *The Open Spectrosc. J.* **2010**, *4*, 16 - 27.

[4] a) V. Schmidts, Technische Universität Darmstadt (Darmstadt), **2013**; b) R. Berger, C. Fischer, M. Klessinger, *J. Phys. Chem. A* **1998**, *102*, 7157-7167.

[5] J. A. Losonczi, M. Andrec, M. W. F. Fischer, J. H. Prestegard, *J. Magn. Reson.* **1999**, *138*, 334-342.

[6] a) N.-C. Meyer, A. Krupp, V. Schmidts, C. M. Thiele, M. Reggelin, *Angew. Chem.* **2012**, *124*, 8459-8463; b) N.-C. Meyer, A. Krupp, V. Schmidts, C. M. Thiele, M. Reggelin, *Angew. Chem. Int. Ed.* **2012**, *51*, 8334-8338; c) P. Giraudeau, T. Montag, B. Charrier, C. M. Thiele, *Magn. Reson. Chem.* **2012**, *50*, S53-S57.

[7] a) T. N. Pham, T. Liptaj, K. Bromek, D. Uhrin, *J. Magn. Reson.* **2002**, *157*, 200-209; b) K. Fehér, S. Berger, K. E. Kövér, *J. Magn. Reson.* **2003**, *163*, 340-346; c) C. M. Thiele, W. Bermel, *J. Magn. Reson.* **2012**, *216*, 134-143.

[8] G. Cornilescu, J. L. Marquardt, M. Ottiger, A. Bax, *J. Am. Chem. Soc.* **1998**, *120*, 6836-6837.

[9] a) C. M. Thiele, V. Schmidts, B. Böttcher, I. Louzao, R. Berger, A. Maliniak, B. Stevensson, *Angew. Chem. Int. Ed.* **2009**, *48*, 6708-6712; b) C. M. Thiele, V. Schmidts, B. Böttcher, I. Louzao, R. Berger, A. Maliniak, B. Stevensson, *Angew. Chem.* **2009**, *121*, 6836-6840.

[10] M. Foroozandeh, R. W. Adams, N. J. Meharry, D. Jeannerat, M. Nilsson, G. A. Morris, *Angew. Chem. Int. Ed.* **2014**, *53*, 6990-6992.

[11] a) B. Yu, H. van Ingen, S. Vivekanandan, C. Rademacher, S. E. Norris, D. I. Freedberg, *J. Magn. Reson.* **2012**, *215*, 10-22; b) B. Yu, H. van Ingen, D. I. Freedberg, *J. Magn. Reson.* **2013**, *228*, 159-165.

[12] T. Reinsperger, B. Luy, *J. Magn. Reson.* **2014**, *239*, 110-120.